

Flashback Characteristics of Syngas-Type Fuels Under Steady and Pulsating Conditions

Final Report

Principal Investigators: Tim Lieuwen

Date Report was issued February 8, 2008

DOE Award Number: DE-FG26-04NT42176

School of Aerospace Engineering

Georgia Institute of Technology

Atlanta, GA 30332-0150

DISCLAIMER:

“This report was prepared as an account of work sponsored by an agency of the United States Government. Neither the United States Government nor any agency thereof, nor any of their employees, makes any warranty, express or implied, or assumes any legal liability or responsibility for the accuracy, completeness, or usefulness of any information, apparatus, product, or process disclosed, or represents that its use would not infringe privately owned rights. Reference herein to any specific commercial product, process, or service by trade name, trademark, manufacturer, or otherwise does not necessarily constitute or imply its endorsement, recommendation, or favoring by the United States Government or any agency thereof. The views and opinions of authors expressed herein do not necessarily state or reflect those of the United States Government or any agency thereof.”

1. ABSTRACT

The objective of this project was to improve understanding and modeling of flashback, a significant issue in low emissions combustors containing high levels of hydrogen. Experimental studies were performed over a range of fuel compositions, flow velocities, reactant temperatures, and combustor pressures to study the factors leading to flashback. In addition, high speed imaging of the flashback phenomenon was obtained. One of the key conclusions of this study was that there existed multiple mechanisms which lead to flashback, each with different underlying parametric dependencies. Specifically, two mechanisms of “flashback” were noted: rapid flashback into the premixer, presumably through the boundary layer, and movement of the static flame position upstream along the centerbody. The former and latter mechanisms were observed at high and low hydrogen concentrations. In the latter mechanism, flame temperature ratio, not flame speed, appeared to be the key parameter describing flashback tendencies. We suggested that this was due to an alteration of the vortex breakdown location by the adverse pressure gradient upstream of the flame, similar to the mechanism proposed by Sattelmayer and co-workers [1]. As such, a key conclusion here was that classical flashback scalings derived from, e.g., Bunsen flames, were not relevant for some parameter regimes found in swirling flames. In addition, it was found that in certain situations, pure H₂ flames could not be stabilized, i.e., the flame would either flashback or blowout at ignition. This result could have significant implications on the development of future high hydrogen turbine systems.

2. TABLE OF CONTENTS

1. ABSTRACT	3
2. TABLE OF CONTENTS	4
3. LIST OF FIGURES	5
4. EXECUTIVE SUMMARY	9
5. PROJECT DESCRIPTION.....	10
6. BACKGROUND.....	10
7. INSTRUMENTATION AND FACILITY.....	15
8. RESULTS AND DISCUSSION	20
9. CONCLUSIONS.....	40
10. REFERENCES.....	40

3. LIST OF FIGURES

Figure 1: Ratio of Vortex Core Size to Nozzle Radius versus Swirl Number map showing vortex breakdown regions [,]. 12

Figure 2: Schematic of flame front with small perturbation (Dashed line: x axis, Dot-dashed line: y axis)...... 14

Figure 3: Dependence of pressure rise upstream of the flame upon flame temperature ratio. 14

Figure 4: Photograph of high pressure combustor facility...... 16

Figure 5: Premixer with swirler, centerbody, radial thermocouples, and centerbody thermocouple...... 17

Figure 6: New Nozzle for Flashback Imaging. 17

Figure 7: Schematic of Optically Accessible Premixer (not to scale, different centerbody lengths were used)...... 18

Figure 8: Primary color mixing scheme used to denote fuel blend composition. 18

Figure 9: Flame front and postulated recirculation zone locations for normal flame (left) and with flame propagated upstream [”slow” flashback] (right). 19

Figure 10: Dependence of flashback ($U_0=4 \text{ m/s}$ or equivalently, premixer velocity= 72 m/s) equivalence ratio upon H_2 mole fraction at reactants temperature 300 K and combustor pressure 1.7 atm. Circled point indicates occurrence of rapid upstream propagation flashback mechanism...... 20

Figure 11: Dependence of flashback ($U_0=2 \text{ m/s}$ or equivalently, premixer velocity= 36 m/s) equivalence ratio upon H_2 mole fraction at reactants temperature 460 K and combustor pressure 4.4 atm. Circled points indicate occurrence of rapid upstream propagation flashback mechanism...... 21

Figure 12: Dependence of range of equivalence ratios for which a stable flame can be achieved upon H_2 percentage. Circle: inlet temperature 300 K, pressure 1.7 atm; Square: inlet temperature 460 K, pressure 4.4atm...... 21

- Figure 13:** Dependence of ϕ at flashback upon percentage of H_2 . Star: $U_0=2$ m/s (premixer velocity = 36 m/s), inlet temperature 300 K, pressure 1.7 atm; Square: $U_0=4$ m/s (premixer velocity = 72 m/s), inlet temperature 300 K, pressure 1.7 atm; Circled points indicate occurrence of rapid upstream propagation flashback mechanism. 22
- Figure 14:** Dependence of $S_{L,0}/U_0$ at flashback upon percentage of H_2 . Star: $U_0=2$ m/s (premixer velocity = 36 m/s), inlet temperature 300 K, pressure 1.7 atm; Square: $U_0=4$ m/s (premixer velocity = 72 m/s), inlet temperature 300 K, pressure 1.7 atm; Circled points indicate occurrence of rapid upstream propagation flashback mechanism. 22
- Figure 15:** Total pressure (mean plus fluctuation) across the flame front. 23
- Figure 16:** Hypothesized flow streamlines in the vicinity of the flame and recirculation bubble. 23
- Figure 17:** Dependence of adiabatic flame temperature at flashback upon percentage of H_2 . $U_0=2$ m/s (premixer velocity = 36 m/s), inlet temperature 460 K, pressure 4.4 atm. Circled points indicate occurrence of rapid upstream propagation flashback mechanism. 24
- Figure 18:** Dependence of adiabatic flame temperature of CH_4 at flashback upon combustion pressure at the same flow rate. Circle: inlet temperature 300 K (premixer velocity range is 36 to 52 m/s); Square: inlet temperature 460 K (premixer velocity range is 58 to 94 m/s). 25
- Figure 19:** ϕ at Flashback versus % H_2 and % CH_4 : $U_0=1.2$ m/s, $T_0=500$ K, and $P=7.1$ atm. 26
- Figure 20:** ϕ at Flashback versus % H_2 and % CH_4 : (a) $T_0=300$ K and $P=1.7$ atm [Circle: $U_0=2$ m/s & Square: $U_0=4$ m/s], (b) $U_0=5.4$ m/s, $T_0=458$ K and $P=4.4$ atm and ϕ at Flashback versus % H_2 , and (c) $U_0=4$ m/s, $T_0=458$ K and $P=4.4$ atm. 27
- Figure 21:** Dependence of Adiabatic Flame Temperature on % H_2 : (a) $U_0=1.2$ m/s, $T_0=500$ K and $P=7.1$ atm, (b) $T_0=300$ K and $P=1.7$ atm [Circle: $U_0=2$ m/s & Square: $U_0=4$ m/s], (c) $U_0=5.4$ m/s, $T_0=458$ K and $P=1.7$ atm, and (d) $U_0=4$ m/s, $T_0=458$ K and $P=4.4$ atm. 28
- Figure 22:** Dependence of Laminar Flame Speed on % H_2 : (a) $U_0=2$ m/s, $T_0=300$ K and $P=1.7$ atm, (b) $U_0=4$ m/s, $T_0=300$ K and $P=1.7$ atm, (c) $U_0=5.4$ m/s, $T_0=458$ K and $P=1.7$

atm, and (d) $U_0= 4$ m/s, $T_0=458$ K and $P=4.4$ atm.	29
Figure 23: Dependence of Estimated Laminar Flame Speed on %H₂: $U_0=1.2$m/s, $T_0=500$K, and $P=7.1$ atm.....	30
Figure 24: Pressure Sweep Data at $U_o=0.96$ m/s (Nozzle $U=17.3$ m/s) and $T_{in}=480$K: (a) T_{ad} [K] versus %H₂ and (b) ϕ versus %H₂ [Square=2 atm, Diamond=3 atm, and Triangle=4 atm] {Circled points indicate that flashback was not well defined}.....	30
Figure 25: CO Flame Anchored in nozzle.	31
Figure 26: Pressure sweep data: T_{ad} vs. combustor pressure, same conditions as Figure 24.....	31
Figure 27: Optically accessible premixer for syngas testing. The blue line represents reactants entering the premixer and the red line represents the direction and location of the combustor. Flashback is noted when the flame propagates in the small quartz tube circled in yellow. [See Figure 6 and Figure 7 for more details in INSTRUMENTATION AND FACILITY section].....	32
Figure 28: Velocity vs. Radial position using Hotwire Anemometer. Hotwire probe was at the tube exit.	32
Figure 29: Velocity vs. Radial position using Hotwire Manometer. Data was taken at 1/8 inch and 1/4 inch depths into the small quartz tube.	33
Figure 30: Velocity vs. axial position using hotwire manometer. Axial position here is in inches.....	33
Figure 31: LDV setup using aluminum oxide particles and a 1” centerbody with a 35 degree swirler and three inch quartz tube.....	34
Figure 32: Axial Velocity vs. Normalized Radial Position. Nozzle velocity is 26 m/s corresponding to the 150psi Hotwire cases above. LDV position was at tube exit.....	34
Figure 33: Sample CH₄ flashback image showing the location of the swirler, centerbody, and combustor adapter.....	35
Figure 34: CH₄ Flashback Propagation (Test 1) at 337 K, 1 atm, and nozzle velocity of 39.8 m/s. Shows the flame propagation sequence zoomed in on the quartz tube [Images are	

0.5 ms apart].....	35
Figure 35: CH₄ Flashback Propagation (Test 2) at 337 K, 1 atm, and nozzle velocity of 39.8 m/s. Shows the flame propagation sequence zoomed in on the quartz tube [Images are 0.5 ms apart].	35
Figure 36: Flame tip position versus time [position in inches, time in ms, and position = 0in was at the inlet to the propagation tube]. Note flame propagation of 6 and 6.3 m/s, respectively between tests 1 and 2.	36
Figure 37: Sample 80% CH₄, 20% H₂ flashback image showing the location of the combustor adaptor, quartz tube, and swirler.	36
Figure 38: 80% CH₄, 20% H₂ flashback at 359 K, 1 atm, and nozzle velocity of 48.83 m/s. Shows the flame propagation sequence zoomed in on the quartz tube. Images are 0.5 ms apart.	37
Figure 39: Flame tip position versus time [position in inches, time in ms, and position = 0in was at the inlet to the propagation tube]. Note flame propagation of 10 m/s.....	37
Figure 40: Propagation velocity vs. %H₂ in the fuel for 290K and 1 atm [Note: where squares $U_{nozzle}=18.8\text{m/s}$ or $U_o=2\text{m/s}$ and diamonds $U_{nozzle}=58.7\text{m/s}$ or $U_o=6.5\text{m/s}$.	38
Figure 41: Adiabatic Flame Temperature (K) and equivalence ratio versus percent H₂ for same conditions as tested in the optically accessible nozzle [Note: where squares $U_{nozzle}=18.8\text{m/s}$ or $U_o=2\text{m/s}$ and diamonds $U_{nozzle}=58.7\text{m/s}$ or $U_o=6.5\text{m/s}$].	38
Figure 42: Laminar flame speed versus percent H₂ for same conditions as tested in the optically accessible nozzle [Note: where squares $U_{nozzle}=18.8\text{m/s}$ or $U_o=2\text{m/s}$ and diamonds $U_{nozzle}=58.7\text{m/s}$ or $U_o=6.5\text{m/s}$.	39

4. EXECUTIVE SUMMARY

Currently, flashback is a major issue in low emissions combustors when utilizing fuels with high H₂ levels – all current DLN installations restrict the levels of hydrogen in the fuel to values that are at least one order of magnitude lower than values contemplated for future systems. The objective of this project is to improve the state of the art in understanding and modeling of flashback. The information gained from this project will lend a better insight into preventing flashback occurrences when using alternative fuels in gas turbine systems.

Extensive efforts were made toward the understanding of flashback of syngas fuels. First, we designed and developed an experimental facility to characterize the flashback. Then, experimental studies were performed over a range of fuel compositions at fixed approach or burned flow velocity, reactant temperature, and combustor pressure at several conditions up to 7.1 atm and 500 K inlet reactants temperature. In certain selected cases, visualizations of syngas flashback were performed using an optically accessible premixer. This allowed for flame visualization and propagation measurement.

One of the key conclusions of this study was that there existed multiple mechanisms which lead to flashback, each with different underlying parametric dependencies. Counter-intuitively, the percentage of hydrogen had far less effect on flashback characteristics, at least for fuels with hydrogen mole fractions less than 60% and for lower combustor pressures. This was due to the fact that two mechanisms of “flashback” were noted: rapid flashback into the premixer, presumably through the boundary layer, and movement of the static flame position upstream along the centerbody. The former and latter mechanisms were observed at high hydrogen and/or higher combustor pressures, and low hydrogen concentrations, respectively. In the latter mechanism, flame temperature, not flame speed, appeared to be the key parameter describing flashback tendencies. We suggested that this was due to an alteration of the vortex breakdown location by the adverse pressure gradient upstream of the flame, similar to the mechanism proposed by Sattelmayer and co-workers [1]. As such, a key conclusion was that classical flashback scalings derived from, e.g., Bunsen flames, may not be relevant for some parameter regimes found in swirling flames. Moreover, with higher pressure tests, it was found that rapid flashback became dominant regardless of the H₂ levels in the fuel. Finally, it was found that in cases of higher pressure/temperature, pure H₂ flames could not be stabilized, i.e., the flame would either flashback or blowout at ignition. This result could have significant implications on the development of future high hydrogen turbine systems.

5. PROJECT DESCRIPTION

This program investigated flashback of high hydrogen syngas fuels. The information gained improved the understanding and modeling of flashback, which is known to be a significant issue in low emissions combustors containing high levels of hydrogen. Current DLN systems restrict the allowable levels of H₂ in the fuel to values that are at least an order of magnitude lower than that being considered for future systems. In cases where the fuel is H₂ rich, it must be burned in diffusion flame combustors which produce high levels of NO_x.

The project consisted of multiple thrusts. First, a systematic design of experiments that formed the test matrix for the experiments performed under this project. Because of the significant number of independent parameters that needed to be examined (e.g., fuel composition, pressure, pre-mixer design), a systematic effort was needed so that the resulting parametric studies were of sufficient breadth and detail, yet still realistic in scope. Then, an extensive series of tests were performed which characterized the dependence of flashback characteristics upon fuel composition, pressure, inlet temperature, and premixer configuration. Particular emphasis was given on elucidating the two flashback mechanisms deduced from these studies, and the parametric sensitivities of these two mechanisms to flow conditions.

6. BACKGROUND

Flame stabilization involves competition between the rates of the chemical reactions and the rates of turbulent diffusion of species and energy. While a significant amount of fundamental understanding of flame propagation and stability characteristics of lean, premixed systems had been gained in conventionally fueled, natural gas-air systems [2], little was known about these issues for alternate gaseous fuels, such as syngas or low BTU fuel mixtures. Furthermore, the majority of the fundamental investigations of the combustion characteristics of these synthetic gases were for non-premixed flame configurations [3,4,5,6,7]. Limited studies had been initiated relatively recent to investigate the characteristics of premixed, hydrogen-enriched methane fuels [8,9,10]. Additional studies were needed to broaden the scope of fuels of interest.

Flashback was used here to describe situations where the flame physically propagated upstream of the region where it was supposed to anchor and into premixing passages that were not designed for high temperatures. Flashback was an issue because of the widely varying flame speeds of candidate fuels. While this was a classical topic that had been extensively investigated [11,12,13], the complexity of the topic increased substantially in swirling flows. In particular, several potential modes of flashback occurred in swirling flows, as discussed in a series of papers by Sattelmayer and co-workers [14,15,16]. They identified three mechanisms for flashback: flashback in the boundary layer, turbulent flame propagation in the core flow, and flashback due to combustion instabilities [17]. The first two mechanisms were captured partially by the laminar and/or turbulent flame

propagation speed. A thorough investigation of boundary layer flashback in syngas fueled Bunsen flames had been detailed by Davu *et al.* [18]. When the local turbulent flame speed exceeded the local flow velocity, the flame could propagate upstream into the premixing section. This issue was complicated by the radial variation in flow velocity, quenching losses, and turbulent flame speed. In the experiments reported here for higher H₂ cases and all higher pressure cases, we got this “rapid” flashback. For other cases, the second mechanism that occurred was a phenomenon Sattelmayer and co-workers referred to as “combustion induced vortex breakdown”. The basic idea was that the flame contributed to vortex breakdown, and therefore a low or negative flow region ahead of it. The flame advanced forward, causing the vortex breakdown region location to advance farther upstream. This process continued as the flame proceeded farther and farther upstream. In this scenario, flashback occurred even if S_T was everywhere less than the flow velocity. As will be discussed below, we believed that a similar phenomenon was occurring in many cases in the tests reported here. However, rather than the flame continuously propagating upstream, we found that the static flame anchoring position monotonically moved upstream, in lower pressure cases, as the mixture fuel/air ratio increased, apparently due to a change in the location of vortex breakdown.

As a result of this work, we propose that this “slow flashback” mechanism occurred due to the fact that the fuel nozzle in many combustors operates in a bi-stable regime of swirling flows. This was illustrated by the figures below, which plotted the qualitative stability diagram for a swirling flow, following Rusak [19]. The left graph plotted a qualitative vortex breakdown stability map, as a function of swirl number and vortex core size. As shown, at low swirl numbers, no vortex breakdown occurred. At very high swirl numbers, vortex breakdown occurred. However, at intermediate values which were typical of those used in practical systems (e.g., ~0.6-1.2) the system had two possible states – no vortex breakdown or vortex breakdown. This was illustrated more abstractly in the right figure which plotted a functional proportional to the energy in the flow. The graph labeled $\omega < \omega_0$ corresponded to the no vortex breakdown state. The graph possessed a single minimum, which corresponded to the steady state flow solution, axial flow. The graph labeled ω_0 corresponded to sitting on the line of the bi-stable region and the next graphs $\omega_0 + \epsilon$ moved into the bi-stable region. Note that *two minima were present, which corresponded to two possible flow solutions*. The graph labeled ω_1 corresponded to sitting on the line of the vortex breakdown region – at this swirl level the initial minima, corresponded to the no vortex breakdown solution that was no longer present. Further increases in swirl lead to only one possible solution state, vortex breakdown.

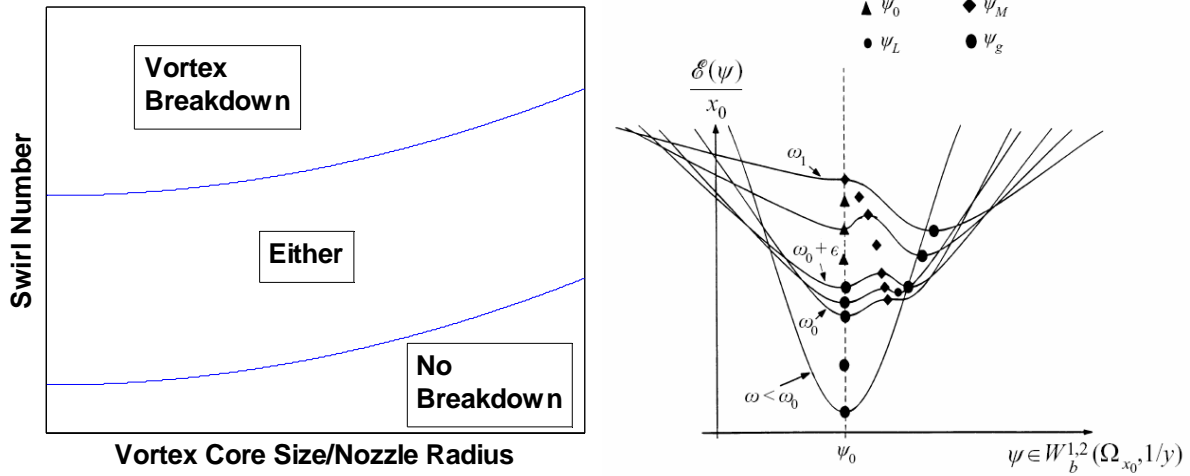


Figure 1: Ratio of Vortex Core Size to Nozzle Radius versus Swirl Number map showing vortex breakdown regions [19, 20].

As noted above, at swirl levels typical of those used in practical systems (e.g., ~ 0.6 - 1.2) the swirling flow possesses two possible dynamic states – no vortex breakdown or vortex breakdown. Basically, we believed that this new flashback mechanism occurs in this bi-stable region and therefore, the regime where practical designs operate. The flow was nominally axial, but could also, if appropriately perturbed, jump over the barrier and find the other energy functional minima corresponding to vortex breakdown.

What then can cause this perturbation to make the flow jump from the purely axial to the breakdown state. It is known that the presence of adverse pressure gradients is destabilizing and can provide this effect. This is apparently the reason why the vortex breakdown location “locks” into the zone just downstream of the rapid expansion in practical combustion systems. This strong adverse pressure gradient provides the impetus for pushing the flow from the axial to the breakdown state at a fixed location. In contrast, it should be noted that the vortex breakdown location is somewhat random and subject to movement and fluctuation in a straight pipel

A key proposal we put forward from this work is that the flame can also provide this perturbation. Specifically, *the adverse pressure gradient in front of the flame provides this perturbation to the flow*. Moreover, the amplitude of the perturbation provided by the flame is proportional to two quantities – the relative angle of the flame and flow and the temperature ratio across the flame. The paragraphs below provides a full analysis demonstrating these two points.

In general a theoretical analysis of flame flow coupling is analytically intractable, due to the fact that it is essentially a nonlinear, free boundary problem, that couples the two nonlinear flow solutions (described by the Navier-Stokes equations) to the nonlinear flame front tracking equation (described by the G equation). As such, we

performed a perturbation analysis which is motivated from the Darrieus-Landau flame stability analysis¹ [21]. This analysis is performed for a flame with small sinusoidal wrinkles of spatial wavenumber k and amplitude D (see Figure 2), with flame temperature ratio $\mathcal{R} = T_b/T_u$. The pressure upstream of the flame equaled its nominal value, plus a small perturbation due to the wrinkle, $P(x) = \bar{P} + P'(x)$. The acceleration of the gases through the flame causes the nominal burned gas pressure to drop, as given by the following expression:

$$\bar{P}_b = \bar{P}_u - (\mathcal{R} - 1) \bar{\rho}_u \bar{U}_u^2 \quad (1)$$

The alteration of the upstream pressure field by the flame wrinkled along the indicated line in the figure below is given by:

$$\frac{P'_u(x)}{\left(\frac{1}{2} \bar{\rho}_u \bar{U}_u^2\right)(kD)} = \frac{-(\mathcal{R} - 1)(\sigma - \mathcal{R})e^{kx}}{2 \left(\mathcal{R} \frac{(\sigma - 1)}{(\sigma + \mathcal{R})} [1 + \sigma] + \left(1 - \frac{\sigma}{\mathcal{R}}\right) \right)} \quad (2)$$

where

$$\sigma = \frac{-\mathcal{R}}{1 + \mathcal{R}} \left[\sqrt{1 + \mathcal{R} + \frac{1}{\mathcal{R}}} - 1 \right] \quad (3)$$

The spatial dependence of the pressure through the flame along the dashed line in Figure 2 was plotted in Figure 15.

¹ Note that this stability theory shows that such a perturbation is unstable. However, the corresponding pressure profiles are correct for the flame front whose instantaneous perturbation amplitude is D .

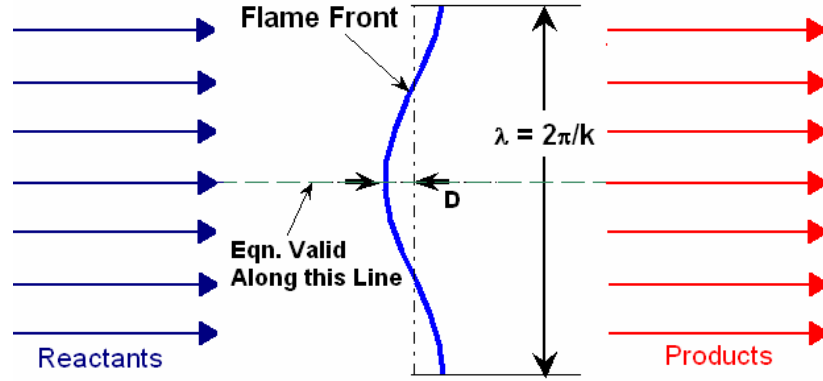


Figure 2: Schematic of flame front with small perturbation (Dashed line: x axis, Dot-dashed line: y axis).

The magnitude of the pressure rise upstream of the flame, indicated in Figure 15, was given by the expression:

$$\frac{\Delta P'}{\left(\frac{1}{2}\rho_u U_u^2\right)(kD)} = \frac{-(\mathfrak{R} - 1)(\sigma - \mathfrak{R})}{2\left(\mathfrak{R}\frac{(\sigma - 1)}{(\sigma + \mathfrak{R})}[1 + \sigma] + \left(1 - \frac{\sigma}{\mathfrak{R}}\right)\right)} \quad (4)$$

The dependence of this pressure rise upon the temperature ratio across the flame was plotted in Figure 3:

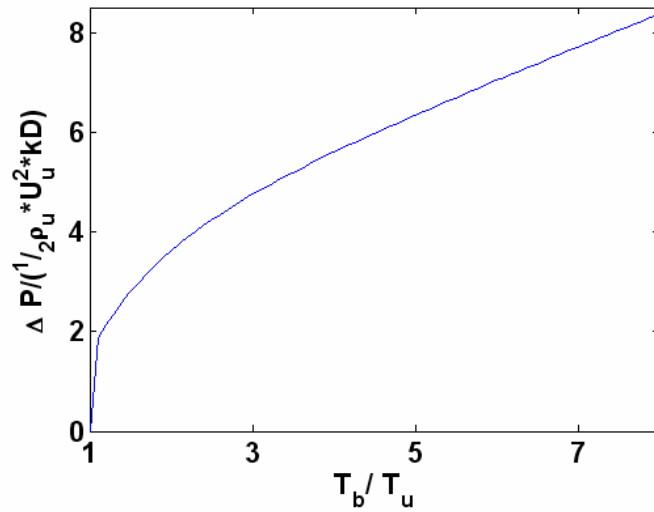


Figure 3: Dependence of pressure rise upstream of the flame upon flame temperature ratio.

This result shows that the adverse pressure gradient ahead of the flame grew monotonically with temperature ratio across the flame, as well as the relative inclination angle of the flame with respect to the flow, related to kD . As such, this provides a possible explanation for our experimental observation that the temperature ratio across the flame, and not the flame speed, was the key parameter controlling the regions where the “slow flashback” mechanism occurred.

The next sections describe the facility and measurements which presented more detailed presentations of the results of the program.

7. INSTRUMENTATION AND FACILITY

Flashback measurements were obtained in a 7.6 cm (3”) diameter quartz tube combustor housed in a pressure vessel, see Figure 4. The premixer was modified with additional instrumentation as needed for the flashback measurements. This premixer was fully modular as the centerbody and swirler could be easily removed and replaced; tests reported here were performed with a single 12 vane, 35° swirler. More details about the facility were in Ref. [22]. Although referred to here as a “premixer”, we actually mixed the fuel and air far upstream to ensure a homogeneous mixture.

Fuels of arbitrary composition were generated with a blending facility that consisted of six mass flow controllers, plumbed to bottles of H_2 , CO , CH_4 , CO_2 , N_2 , and/or any other arbitrary fuel.

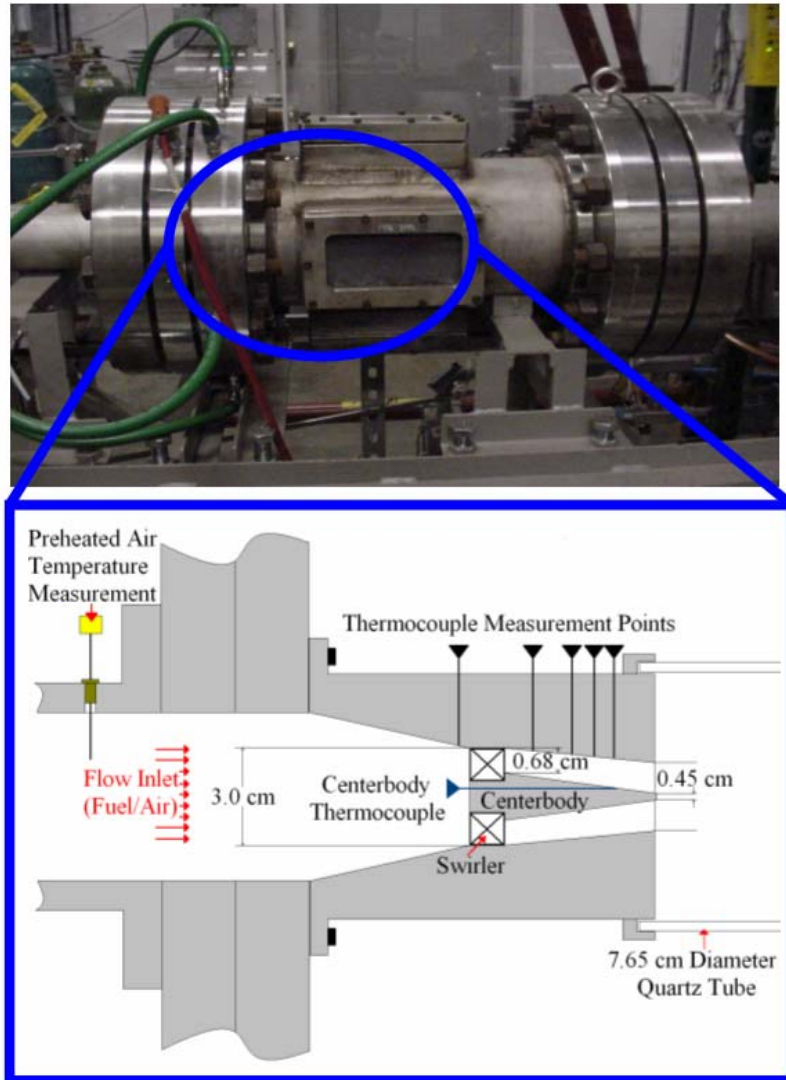


Figure 4: Photograph of high pressure combustor facility.

To detect flashback, a total of fifteen measurement points were arranged on the outer wall of the premixer, as shown below, five in a row at successive axial locations, with three locations at successive 120° azimuthal positions at each axial location. Also, a thermocouple was mounted on the surface of the centerbody, approximately 1.9 cm from the tip (see Figure 5). An additional thermocouple was located upstream of the premixer (see Figure 4).

Figure 5 showed the premixer with the three rows of five thermocouples. The first three thermocouples, along with the centerbody thermocouple, were used in determining flashback. The two end thermocouples were only used in some cases to determine the distance of flashback into the premixer. Once the flame moved upstream, it was sensed by a thermocouple, triggering a flashback alarm. The mixture was quickly leaned out, and the flashback procedure was repeated. Note that target temperatures were chosen based upon prior tests and visual observations of the flame shape and behavior. In other words, in cases where the “slow flashback” mechanism was

observed, defining the point of flashback was somewhat arbitrary as it was really a continuous process, as opposed to a discrete one. However, for the rapid flashback cases, such as observed with high hydrogen fuels or at higher pressure, the centerbody thermocouple was used to detect flashback by exhibiting a large jump in temperature (+150°F or more).

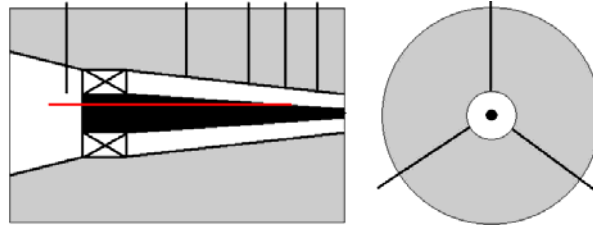


Figure 5: Premixer with swirler, centerbody, radial thermocouples, and centerbody thermocouple.

For tests where imaging of the dynamic flashback process was examined, an optically accessible premixer was used that had a 3 inch long quartz tube upstream of the nozzle dump plane. Figure 6 and Figure 7 illustrated the nozzle used in these tests. Essentially, this was a similar setup to the first nozzle used, except there was not a converging section with a centerbody, which equated to a constant cross-sectional area nozzle. Instead in this case, the cross-sectional area was constant until the flame would propagate upstream to the centerbody, at this point, the area was decreased due to the presence of the centerbody. Flashback images were captured for these tests using a Phantom intensified high speed, black and white camera.

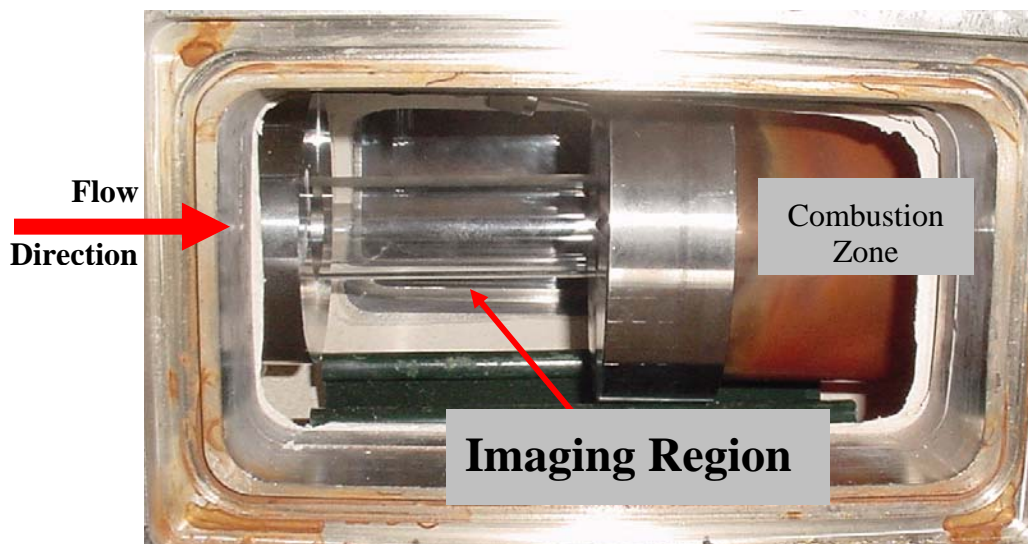


Figure 6: New Nozzle for Flashback Imaging.

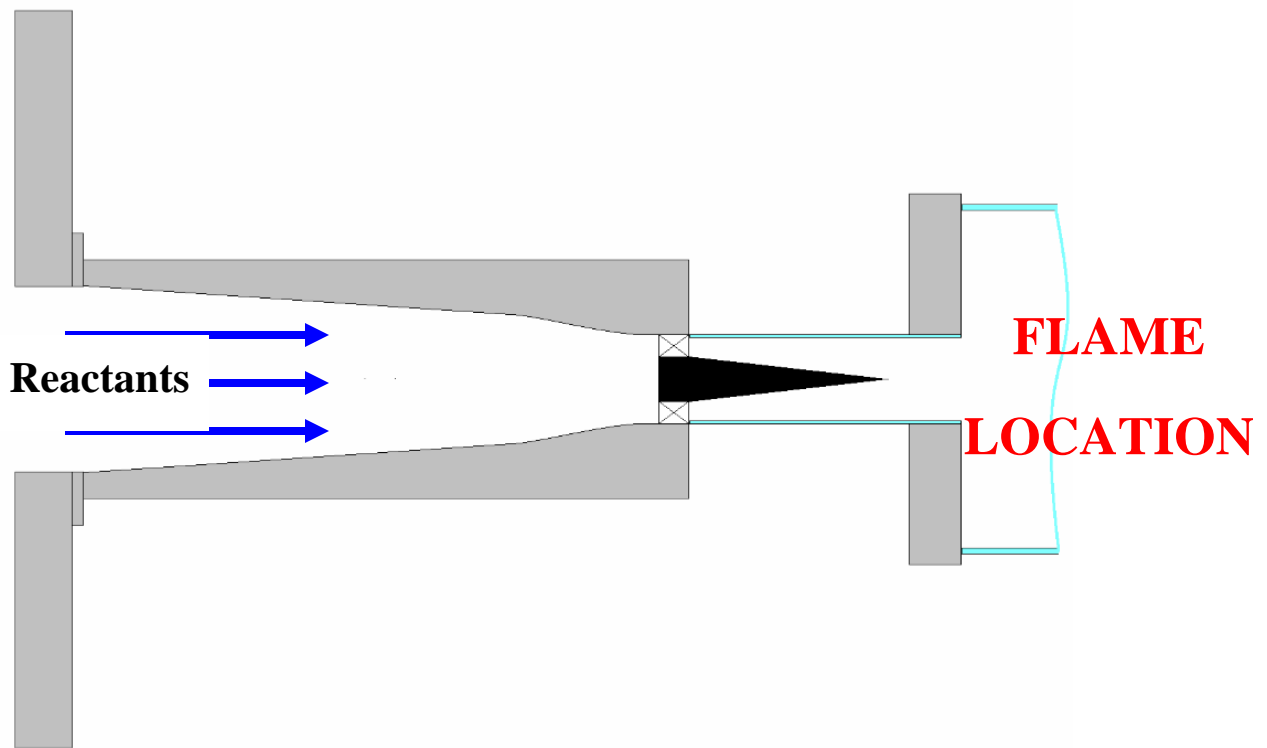


Figure 7: Schematic of Optically Accessible Premixer (not to scale, different centerbody lengths were used).

Furthermore, in order to facilitate presentation of results, we represented the mixture composition of $H_2/CO/CH_4$ by an assigned color. Primary colors at the three vertices were used to represent each fuel constituent, where red, yellow, and blue denoted H_2 , CO , and CH_4 , respectively. This was illustrated in the figure below. Unfortunately, Figure 8 will be difficult to interpret if reproduced in grayscale.

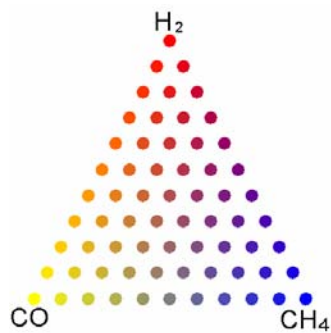


Figure 8: Primary color mixing scheme used to denote fuel blend composition.

The basic test sequence was to operate at various fuel compositions in $H_2/CO/CH_4$ space, such as depicted in the figure above. At each fuel composition, the mixture equivalence ratio was adjusted at a constant unburned

velocity until the mixture flashed back. Obtaining this data was complicated by the need to keep the approach flow velocity, combustor pressure, and mixture temperature constant across the range of fuel compositions. As such, fixing the relative fuel compositions required simultaneously adjusting the air and three fuel flow rates in order to keep a constant approach flow velocity. In addition, due to variations in mixture burned gas temperature, maintaining a constant combustor pressure required simultaneous adjustment of the back pressure valve. Finally, variations in molar volume of the fuel necessitated adjusting the air temperature in order to maintain a constant reactant temperature. For the data shown in the Results section, the approach flow velocity, pressure, and temperature remained constant to within 2%, 5%, and 20 K of their quoted values.

Combustor unburned flow velocities which were quoted here equaled the mass flow rate divided by the unburned gas density and combustor area – this was the combustor velocity if there were no flame. It should be emphasized that this was purely a reference velocity, as the actual flow velocities may have been different. The burned gas velocity simply equaled this velocity multiplied by the theoretical temperature ratio across the flame. The velocity at the premixer exit, relevant for the flashback data, equaled the unburned flow velocity multiplied by an area factor of 18.

It has been emphasized that applying a consistently uniform definition of flashback was complicated by the fact that the manner in which the flame flashed back varied with composition. Different flashback mechanisms were found for different fuel compositions. For low H_2 mixtures and lower combustor pressure, the flame anchoring location moved gradually upstream (along the centerbody) with increased equivalence ratio, see Figure 9. In other words, flashback was not a discontinuous phenomenon, where the flame actually propagated upstream into the premixer in a rapid manner. For these cases, flashback was defined here as the point where the thermocouple closest to the exit plane of the premixer reached 450K and 505K for the 300K and 460K reactant preheat cases, respectively.

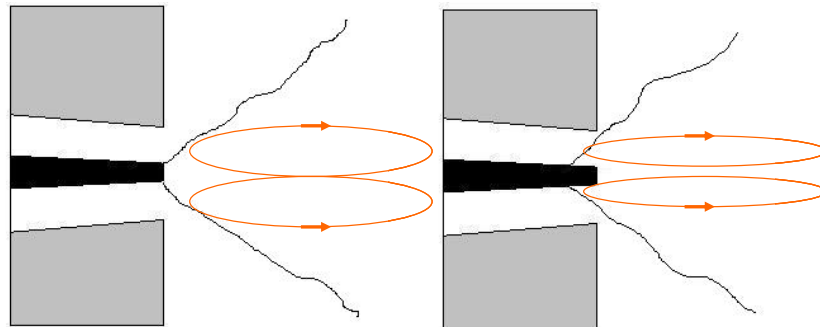


Figure 9: Flame front and postulated recirculation zone locations for normal flame (left) and with flame propagated upstream [’slow’ flashback] (right).

However, for high H_2 mixtures and cases where the combustor pressure was 7.1 atm, flashback occurred very abruptly – triggered by only a slight change in mixture stoichiometry (~ 0.05 or less). The flame very rapidly propagated upstream, sometimes all the way through the swirler where it triggered the thermocouple upstream of the

premixer. Additionally, for the optically accessible premixer, the flame flashback occurred rapidly as well and the flame was viewed propagating completely to the downstream side of the swirler. From these sequences of images, the flame propagation speed was calculated as well.

8. RESULTS AND DISCUSSION

Figure 10 and Figure 11 illustrate typical lower pressure results showing the dependence of the flashback boundaries upon the mole fraction of H_2 in the fuel. The circled points indicate points where flashback occurred very rapidly. For the remainder of the points, “flashback” corresponded to the upstream movement of the flame stabilization point, illustrated in Figure 9. Note that the rapid upstream propagation mechanism occurred at only the highest hydrogen concentration in the low preheat case, and when the percentage of H_2 was greater than 60% in the preheated case.

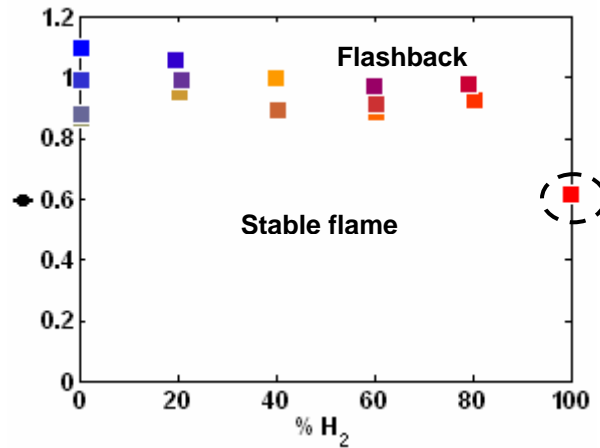


Figure 10: Dependence of flashback ($U_0=4 \text{ m/s}$ or equivalently, premixer velocity= 72 m/s) equivalence ratio upon H_2 mole fraction at reactants temperature 300 K and combustor pressure 1.7 atm. Circled point indicates occurrence of rapid upstream propagation flashback mechanism.

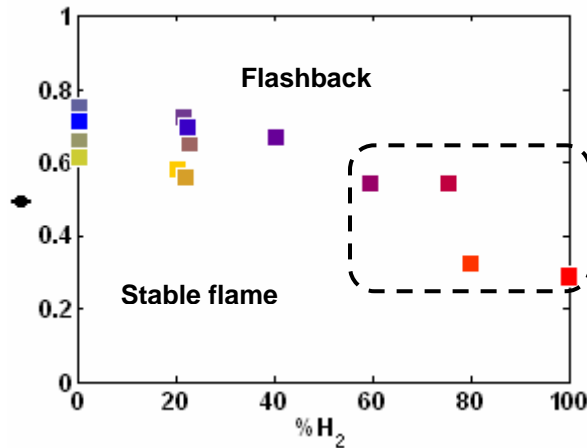


Figure 11: Dependence of flashback ($U_0=2 \text{ m/s}$ or equivalently, premixer velocity= 36 m/s) equivalence ratio upon H_2 mole fraction at reactants temperature 460 K and combustor pressure 4.4 atm. Circled points indicate occurrence of rapid upstream propagation flashback mechanism.

Although these data were obtained at somewhat different premixer velocities (however, the flashback limits did not change significantly with velocity), they were plotted together to illustrate the different sensitivities of these two phenomenon to hydrogen concentration. The flashback result was almost independent of percentage of H_2 , whereas the blowoff equivalence ratio was a very strong function of hydrogen levels, which changed by a factor of almost three in the first figure.

The range of stable operation (i.e., the equivalence ratio range between flashback and blowoff) exhibited a non-monotonic dependence upon $\% \text{H}_2$. For low levels of H_2 addition, this stability range was enhanced, especially for the lower reactant temperature case. However, it was actually decreased at the highest hydrogen levels, due to the propensity of high H_2 mixtures to flashback, see Figure 12 .

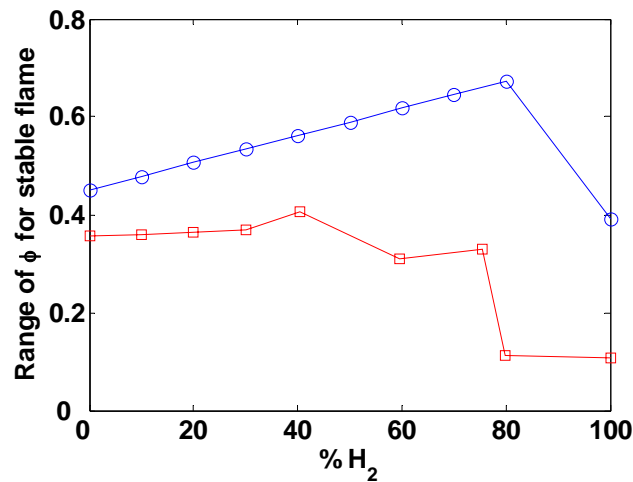


Figure 12: Dependence of range of equivalence ratios for which a stable flame can be achieved upon H_2 percentage. Circle: inlet temperature 300 K, pressure 1.7 atm; Square: inlet temperature 460 K, pressure 4.4atm.

A major effort has been the consideration of how to correlate the flashback data. Figure 13 plots the dependence of the adiabatic flame temperature upon H_2 concentration at two unburned flow velocities. Notice how this flame temperature correlation collapsed much of the variability present in the corresponding flashback equivalence ratio, see Figure 10 and Figure 11, at a fixed H_2 level and varying CO/CH_4 ratio. Furthermore, notice that for all the “slow flashback” cases, flashback occurred at nearly a constant value of flame temperature. As expected, the flame flashed back at lower equivalence ratios at the lower unburned flow speeds; however, this variation was not very significant and, furthermore does not correspond to a similar ratio of flame speeds.

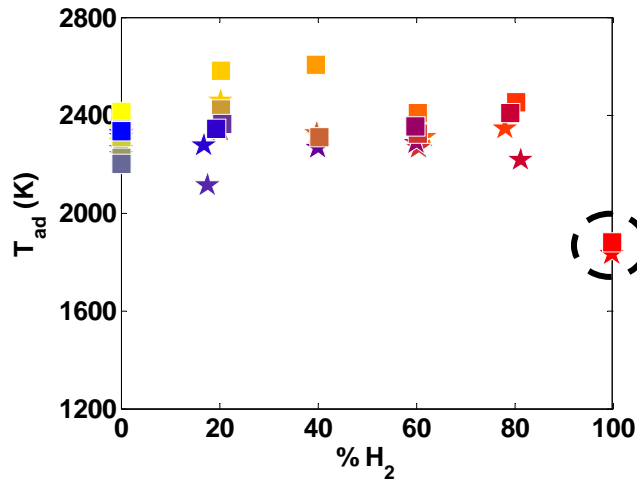


Figure 13: Dependence of ϕ at flashback upon percentage of H₂. Star: $U_0 = 2$ m/s (premixer velocity = 36 m/s), inlet temperature 300 K, pressure 1.7 atm; Square: $U_0 = 4$ m/s (premixer velocity = 72 m/s), inlet temperature 300 K, pressure 1.7 atm; Circled points indicate occurrence of rapid upstream propagation flashback mechanism.

Furthermore, correlations of these results with laminar flame speed, see Figure 14, increased the spread of the data, indicating that laminar flame speed was not an important parameter describing flashback limits.

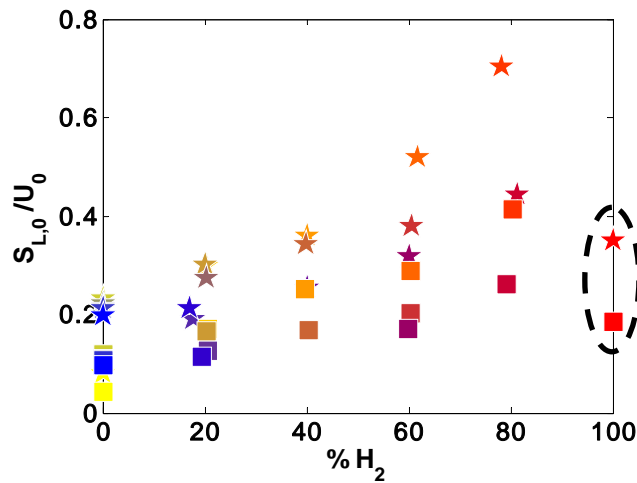


Figure 14: Dependence of S_{L_0}/U_0 at flashback upon percentage of H₂. Star: $U_0 = 2$ m/s (premixer velocity = 36 m/s), inlet temperature 300 K, pressure 1.7 atm; Square: $U_0 = 4$ m/s (premixer velocity = 72 m/s), inlet temperature 300 K, pressure 1.7 atm; Circled points indicate occurrence of rapid upstream propagation flashback mechanism.

We believe that these results supported the assertions of Sattelmayer and co-workers regarding the impact of combustion on the vortex breakdown bubble. It was known that the vortex breakdown location favored regions of adverse pressure gradients, such as rapid flow expansions or equivalently, flow divergence [23]. In the same

way, inclined flame fronts caused divergence of the upstream flow – as such, the flow upstream of the flame was actually decelerating and there was an adverse pressure gradient – even though the flow subsequently accelerated through the flame itself and the pressure drops. Unfortunately, this pressure rise upstream of the flame was very difficult to calculate. We used basic scaling analysis and reference to scaling laws from weakly perturbed flames to show that it scaled with the temperature ratio across the flame, $f(T_b/T_u-1)$. For example, see the analysis in the first section of this report. A result from this analysis showed the spatial variation of the pressure through the flame is plotted in Figure 15. The key point to note from this figure is that convex flame orientation to the flow caused the pressure to actually rise upstream of the flame, followed by the pressure drop across the flame. Note that if the flame were perfectly normal to the flow, there is no pressure rise upstream of the flame.

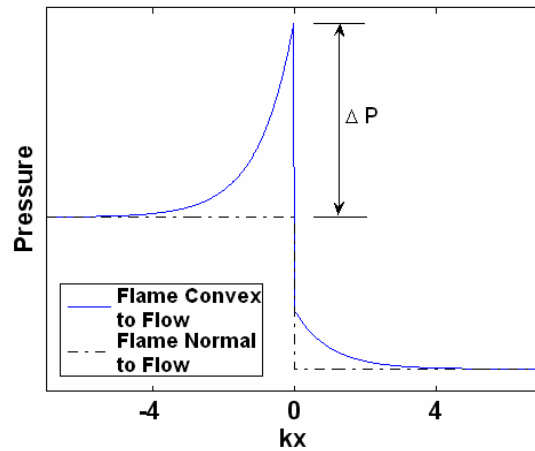


Figure 15: Total pressure (mean plus fluctuation) across the flame front.

Our argument regarding this slow flashback mechanism is better understood with reference to Figure 16, which showed the hypothesized streamlines in the vicinity of the flame and recirculation bubble in more detail.

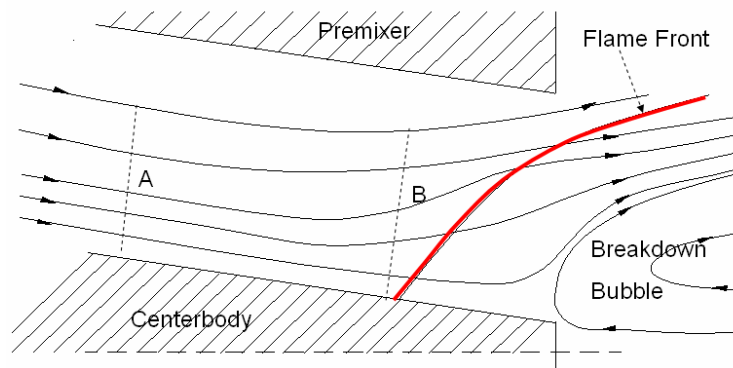


Figure 16: Hypothesized flow streamlines in the vicinity of the flame and recirculation bubble.

The conditions under which the recirculation bubble began to move backward into the premixer, so that there was actually reversed flow in the premixer, is understood by reference to the pressure drop in the premixer, $P_A - P_B$, where the locations “A” and “B” were illustrated in the figure above.

$$\frac{P_A - P_B}{P} = \frac{U_u^2}{RT_u} \left[C_D(\text{Re}, S) - \left(\frac{A_A}{A_B} \right)^2 - f \left(\frac{T_b}{T_u} - 1 \right) \right] \quad (5)$$

where C_D and (A_A/A_B) denoted the contribution to the pressure drop due to viscous losses and the cross-sectional area change, respectively. As indicated, C_D was a function of Reynolds, Re , and swirl number, S . The burned and unburned gas properties were represented by u and b . Presumably, flow instability and vortex breakdown tendencies were enhanced as $P_A - P_B$ decreased, which became more likely as T_b/T_u increased.

The results in Figure 13 are consistent with this picture. These results were obtained with a fixed upstream flow velocity and temperature, and a nearly constant Reynolds number – the only variable that changed was the gas composition. Recall that the one high H_2 point corresponds to a different flashback mechanism. The nearly constant value of T_b at which flashback occurred suggests that the vortex bubble moved into the premixer when $P_A - P_B$ became small enough or negative.

In the same way, there is relatively little change in the flame temperature at flashback with H_2 concentration at a higher pressure and reactant temperature case, as shown in Figure 17. Note that the range of hydrogen levels over which the fast flashback mechanism occurred expanded here.

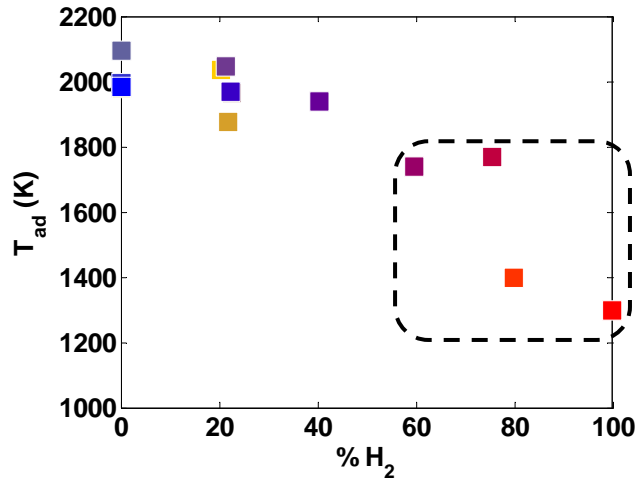


Figure 17: Dependence of adiabatic flame temperature at flashback upon percentage of H_2 . $U_0=2 \text{ m/s}$, (premixer velocity = 36 m/s), inlet temperature 460 K, pressure 4.4 atm. Circled points indicate occurrence of rapid upstream propagation flashback mechanism.

This argument also explains the measured pressure dependence of flashback limits. According to Eq.(5), the relative pressure change was independent of pressure – note that this was what we also observed in tests at two different preheat temperatures, see Figure 18. However, as shown in results at 7.1 atm, T_{ad} no longer stayed constant as manifested from these lower pressure results.

These data presented here also indicates that the flashback temperature decreases with increased unburned gas temperature – i.e., T_b/T_u decreased from 7.6 at $T_u=300$ K to 4.3 at $T_b=460$ K. Thus, the temperature ratio stayed nearly constant with variations in pressure, flow velocity, and fuel composition, but not with unburned gas temperature.

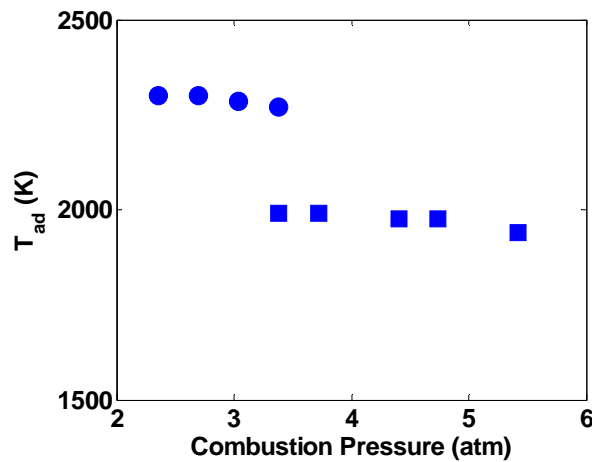


Figure 18: Dependence of adiabatic flame temperature of CH_4 at flashback upon combustion pressure at the same flow rate. Circle: inlet temperature 300 K (premixer velocity range is 36 to 52 m/s); Square: inlet temperature 460 K (premixer velocity range is 58 to 94 m/s).

To further establish whether the key parameter determining the slow flashback proclivity of the flame was dominated by the temperature ratio across the flame, as opposed to the flame speed, we performed a careful test with a high CO mixture, where the equivalence ratio at which the flame temperature peaked, $\phi=1.05$, was well separated from where the flame speed peaked, $\phi=1.24$. The flame position was monitored visually, as well as the centerbody flashback thermocouple. These tests showed that as the fuel-air ratio was swept from lean to rich, the flame moved farther into the premixer and occupied the farthest upstream point at the fuel/air ratio corresponding to maximum flame temperature. Further increases in fuel/air ratio corresponded to conditions where the flame speed was still increasing but the flame temperature was decreasing, resulted in the flame moving back out of the premixer. This result seemed to clearly show that upstream propagation of the flame closely correlated with the mixture's flame temperature, not its flame speed.

Further results of flashback studies on $\text{CO}/\text{H}_2/\text{CH}_4$ mixtures with preheated reactants and raised combustor

pressure were examined at 7.1 atm and 500K, as well as, a set where several fuel combinations were examined at a variety of combustor pressures with constant unburned flow velocity and preheat temperature. Thus, the conditions chosen for the latter data set were preheated temperatures of 480K and nozzle velocity of 17.3 m/s with combustor pressures of 2, 3, and 4 atm. The fuel mixtures used were pure CO, pure CH₄, 95%/5% H₂/CH₄, 50/50 CH₄/CO, 50/50 CH₄/H₂, and 50/50 H₂/CO.

For all the flashback data sets at preheated reactant temperatures and higher combustion pressures, Figure 19-Figure 23 plots these results in terms of equivalence ratio, T_{ad} , and S_L at which flashback occurred. This included the higher pressure data set discussed in the prior paragraph. With all data compiled together, all prior discussed trends are compared in the below section. Note that for some cases, S_L data is not shown because Chemkin would not converge on many all the cases because the equivalence ratio was quite low. Figure 23 uses an estimate of S_L for the 7.1atm/500K case using $S_L^2 \propto \alpha/\tau_{chem}$, where the chemical time and thermal diffusivity are scaled using residence times at blowoff using *AURORA*.

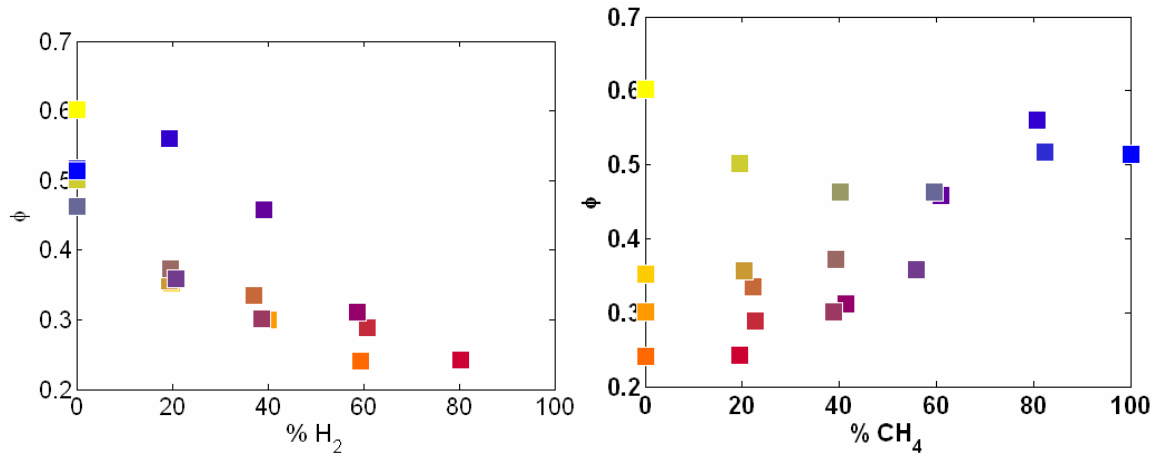


Figure 19: ϕ at Flashback versus %H₂ and % CH₄: $U_0=1.2\text{m/s}$, $T_0=500\text{K}$, and $P=7.1\text{ atm}$.

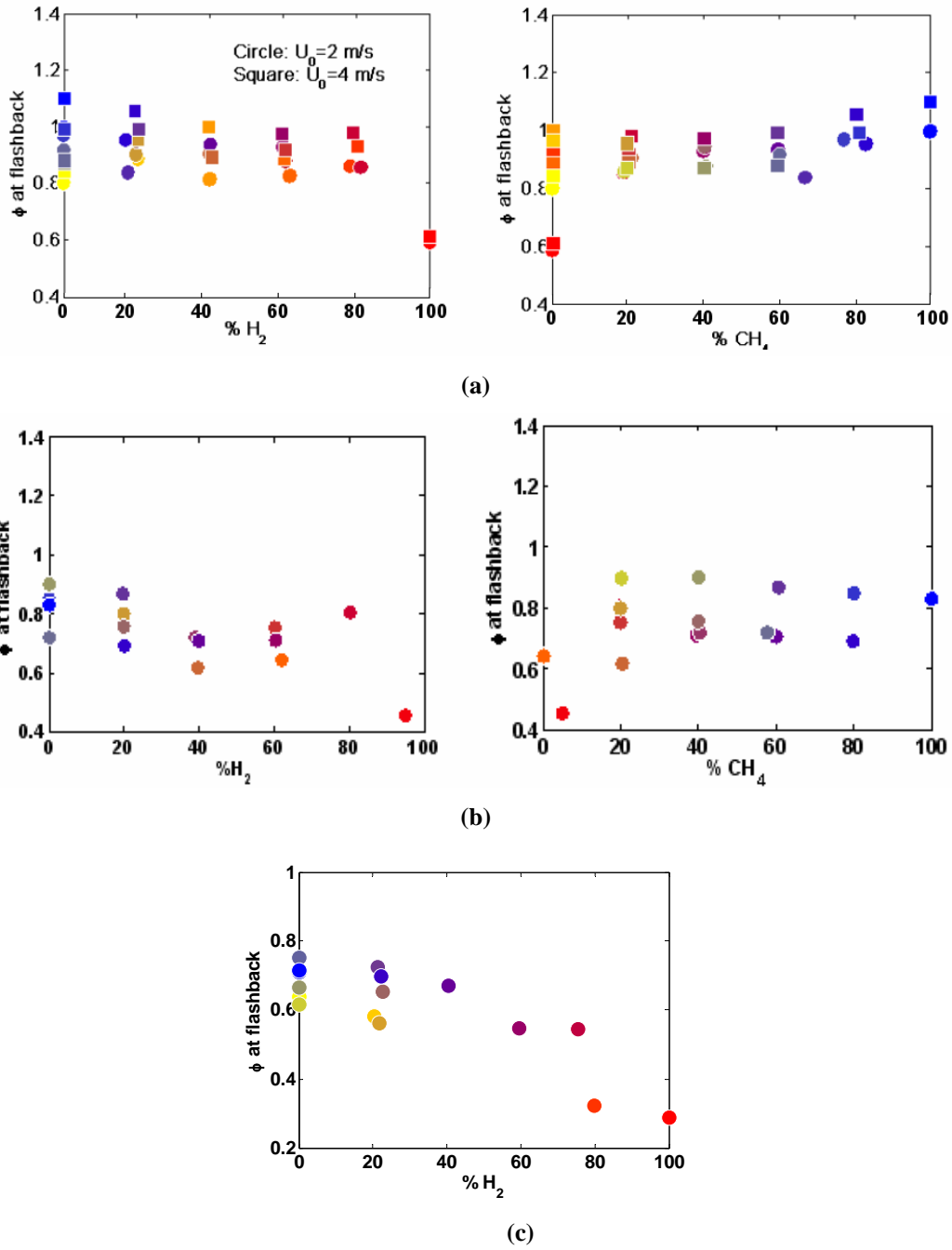


Figure 20: ϕ at Flashback versus $\% \text{H}_2$ and $\% \text{CH}_4$: (a) $T_0=300\text{K}$ and $P=1.7\text{ atm}$ [Circle: $U_0=2\text{ m/s}$ & Square: $U_0=4\text{ m/s}$], (b) $U_0=5.4\text{ m/s}$, $T_0=458\text{K}$ and $P=4.4\text{ atm}$ and ϕ at Flashback versus $\% \text{H}_2$, and (c) $U_0=4\text{ m/s}$, $T_0=458\text{K}$ and $P=4.4\text{ atm}$.

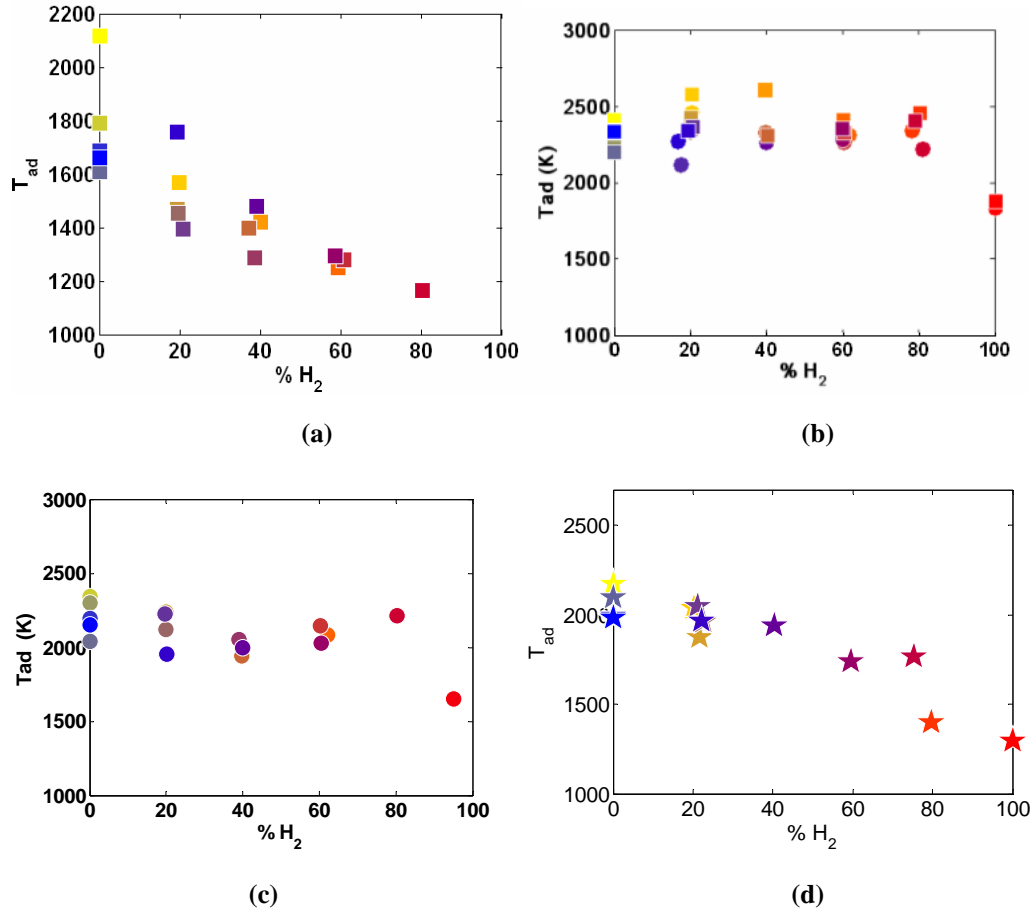


Figure 21: Dependence of Adiabatic Flame Temperature on $\% H_2$: (a) $U_0 = 1.2$ m/s, $T_0 = 500$ K and $P = 7.1$ atm, (b) $T_0 = 300$ K and $P = 1.7$ atm [Circle: $U_0 = 2$ m/s & Square: $U_0 = 4$ m/s], (c) $U_0 = 5.4$ m/s, $T_0 = 458$ K and $P = 1.7$ atm, and (d) $U_0 = 4$ m/s, $T_0 = 458$ K and $P = 4.4$ atm.

From the previous three figure sets (Figure 19-Figure 21), the dependence on equivalence ratio and T_{ad} diminishes as the pressure and temperature increased. It is not as prevalent with the 4.4 atm/458 K case, but with the new 7.1 atm/500 K set, it was very clear during testing that the mode of flashback changed to favoring the rapid mode and the determination of the flashback point changed from a T_{ad} dependence. Note that the rapid flashback is very clear in the 7.1 atm/500 K data. The centerbody thermocouple was utilized for determining the exact point of flashback. A temperature change of 150 to +600 $^{\circ}$ F was noted for all cases for an equivalence ratio change of 0.05 or less. The nozzle velocity for the highest pressure case is lower than the lower pressure cases; however, this lower velocity will be shown later in the results to not be the factor that changed the mode of flashback, it was the pressure increase.

Moreover, the 7.1 atm/500 K did not include pure H_2 because a stable flame was not found. No matter the flow speed or equivalence ratio, the flame would flashback or blow off as soon as pressure was increased from ignition (~ 2 atm) to 7.1 atm. The occurrence was even worse (from a flashback standpoint) if ignition was

attempted at 7.1 atm. This was a significant observation that could have important ramifications in the design of future high hydrogen combustion systems. Attention to high H₂ must be given not only during operation, but during the ignition process as well.

For the laminar flame speed correlation of the data (Figure 22 and Figure 23), all data showed that S_L was not the proper way of correlating flame flashback over the range of fuel compositions. Moreover, in the latter figure, the flame speed was estimated and not the actual numbers from Chemkin. Clearly the better parameter for correlating these data should be using the turbulent flame speed, S_T , but very little of these data exist for syngas mixtures.

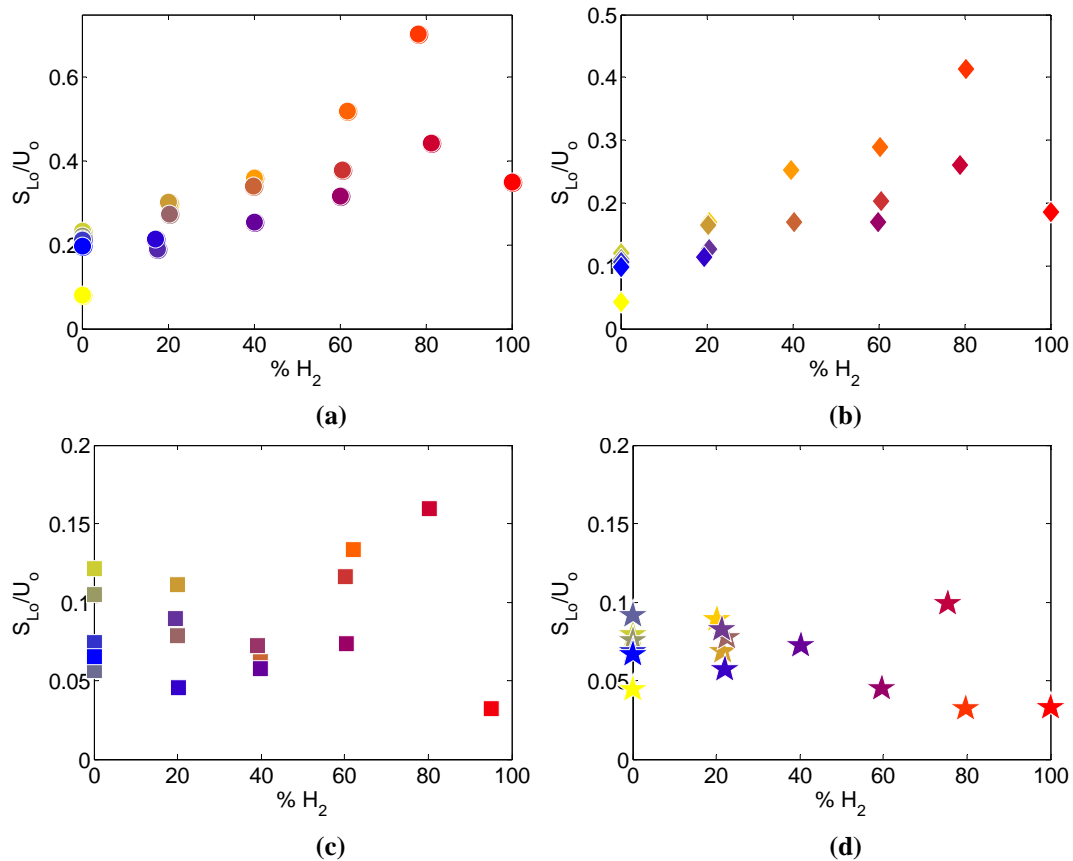


Figure 22: Dependence of Laminar Flame Speed on %H₂: (a) $U_0=2\text{m/s}$, $T_0=300\text{K}$ and $P=1.7\text{ atm}$, (b) $U_0=4\text{m/s}$, $T_0=300\text{K}$ and $P=1.7\text{ atm}$, (c) $U_0=5.4\text{ m/s}$, $T_0=458\text{K}$ and $P=1.7\text{ atm}$, and (d) $U_0=4\text{ m/s}$, $T_0=458\text{K}$ and $P=4.4\text{ atm}$.

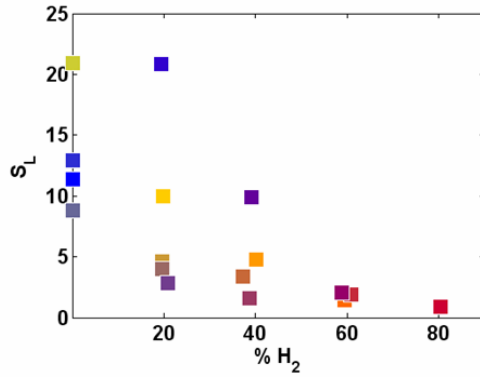


Figure 23: Dependence of Estimated Laminar Flame Speed on %H₂: U₀=1.2m/s, T₀=500K, and P=7.1 atm.

To better understand pressure/Reynolds number effects (note that the Reynolds number scales with the pressure if the flow velocity and temperature were kept constant), pressure sweep data were obtained at constant velocity and preheat temperature. Figure 24 plots the adiabatic flame temperature and equivalence ratio for this case. Note that we were not able to stabilize pure H₂ flames to examine flashback, corresponding to the same problem that was previously described where the flame would flashback or blow off but never became stable. Also, the very high CO cases were not clearly defined as flashback as per our temperature requirements; however, the flame visually was inside the nozzle (see Figure 25). As before, these cases at lower pressures, even with much lower velocities, flashed back with a slower mode. This shows that pressure did affect the flashback occurrence in the previously described data at 7.1 atm and not just the fact that it was at lower flow velocities. As the pressure went up to 4 atm, the flashback mode transitioned to the more rapid flashback. Figure 26 shows that as the pressure was increased, the flashback flame temperature did not change greatly, excluding the CO points; however, again we did notice visually that the mode of flashback changed. This was counter to the 7.1 atm data that showed T_{ad} dependency decreased as pressure increased. This suggests that the dependency change occurred at combustor pressures between 4 and 7.1 atm.

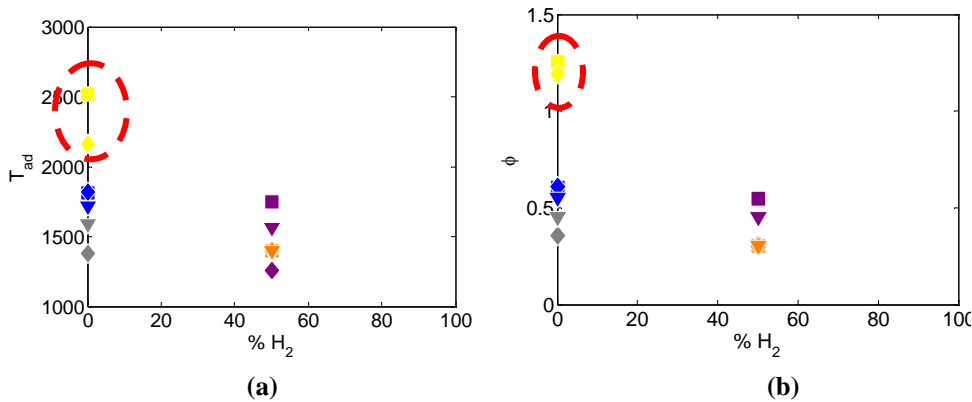


Figure 24: Pressure Sweep Data at U_o=0.96 m/s (Nozzle U=17.3 m/s) and T_{in}=480K: (a) T_{ad} [K] versus %H₂ and (b) φ versus %H₂ [Square=2 atm, Diamond=3 atm, and Triangle=4 atm] {Circled points indicate that flashback was not well defined}.



Figure 25: CO Flame Anchored in nozzle.

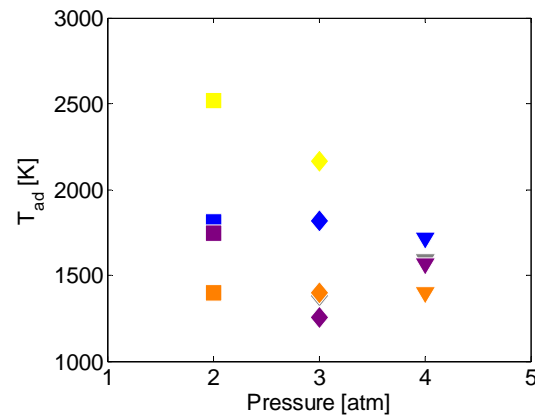


Figure 26: Pressure sweep data: T_{ad} vs. combustor pressure, same conditions as Figure 24.

Furthermore, high speed images of CO/H₂/CH₄ mixtures with the optically accessible premixer under pressurized conditions were examined. This was performed in the same test rig as all the other flashback tests; however, with the optically accessible nozzle design. With this setup, the centerbody was very small/short (only ~1 inch long compared to ~3.5 inches for the first nozzle configuration), as well as, the nozzle no longer had a converging section due to minimizing image distortion. Figure 27 is a picture of the premixer as it was located in the test rig with a window removed. Note that a small H₂ torch was used for ignition and the orange colored tube was a recycled tube from previous flashback testing since flame visualization was not important in the primary combustion zone.

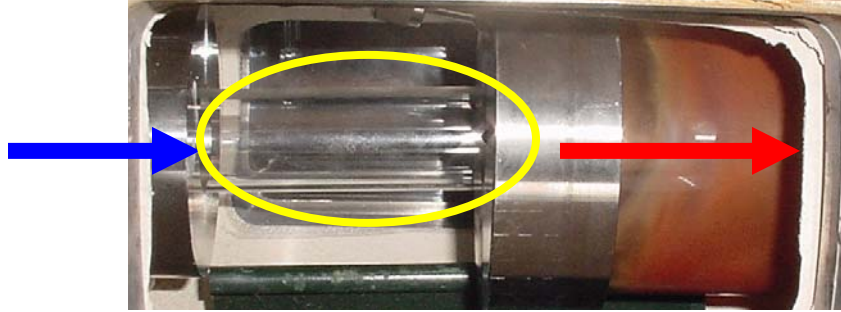


Figure 27: Optically accessible premixer for syngas testing. The blue line represents reactants entering the premixer and the red line represents the direction and location of the combustor. Flashback is noted when the flame propagates in the small quartz tube circled in yellow. [See Figure 6 and Figure 7 for more details in INSTRUMENTATION AND FACILITY section].

Before discussion of the experimental results from the optically accessible premixer, it is important to have knowledge about the flow field of the optical premixer. Importantly, the current portion of the results overviews the investigation of the velocity distribution inside and outside of the optically accessible premixer nozzle. The goal of these analyses was to characterize the recirculation zones near the tip of the small quartz tube. The first part of the examination began with using a traverse with a hotwire probe attached to take a precise radial sweep of the flashback tube, Figure 28. A few important things to note were that the general profile was the same despite changes in flow velocity (inlet pressure) and the hotwire dies not indicate a negative flow velocity due to absolute measurements. If there was, in fact, a reversal of axial velocity, two sharp dips to zero velocity would have been expected somewhere on the graph. It is possible that the traversing of 2mm increments was too coarse to show this phenomenon. In addition, the suction point may not have been completely at the exit, but rather slightly inside the exit.

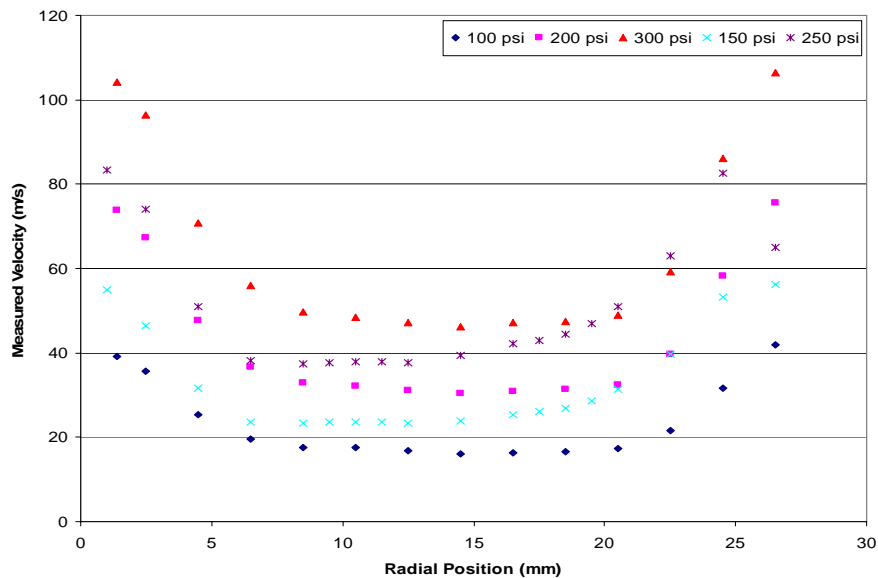


Figure 28: Velocity vs. Radial position using Hotwire Anemometer. Hotwire probe was at the tube exit.

A radial sweep was also completed at 1/8" and 1/4" depths into the small quartz tube (Figure 29). Neither graph showed two drops to zero as would be expected for reversed flow. Either the grid was too coarse or the hotwire was picking up too much non-axial flow.

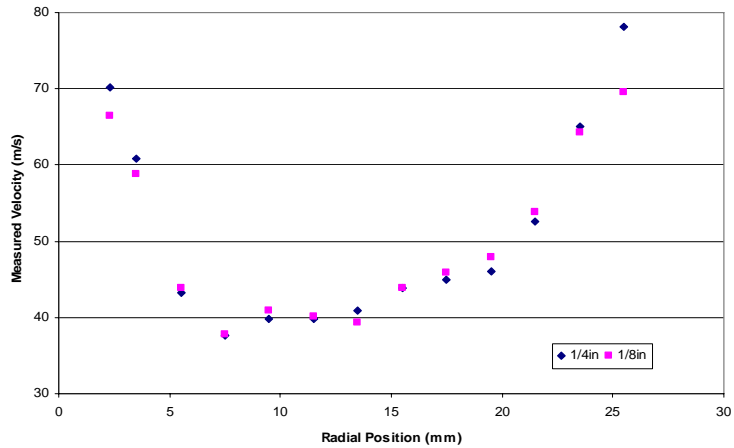


Figure 29: Velocity vs. Radial position using Hotwire Manometer. Data was taken at 1/8 inch and 1/4 inch depths into the small quartz tube.

Additional testing was performed in order to characterize the flow inside the tube along the centerline. If there was a position where recirculation occurred, then a minimum value in the axial velocity would occur somewhere along the sweep. According to Figure 30, suction may had begun near 0.9" into the small quartz tube for this setup. Due to the uncertainty of the hotwire measurements and complicated flow structure inside the tube, Laser Doppler Velocimetry was used to verify the apparent suction that was believed to occur at the tube exit (Figure 31). The LDV measurements shown in Figure 32 verified a portion of the exit flow contained recirculating flow.

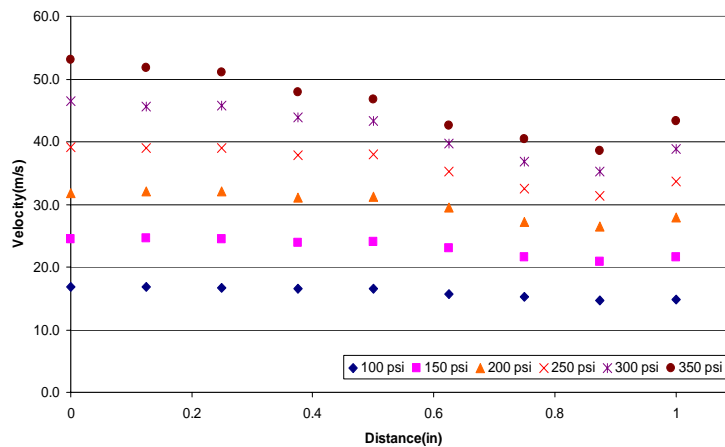


Figure 30: Velocity vs. axial position using hotwire manometer. Axial position here is in inches.

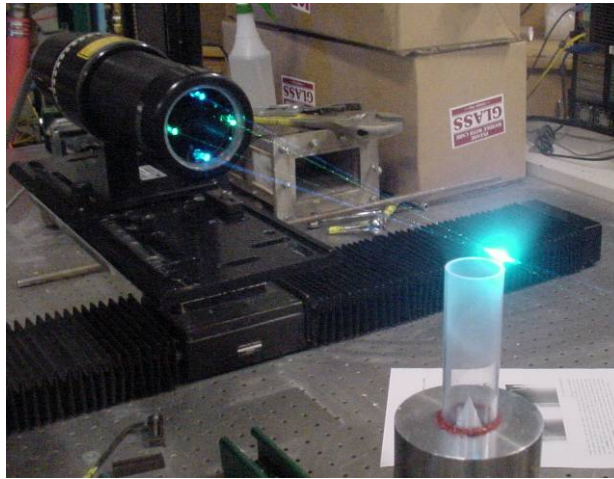


Figure 31: LDV setup using aluminum oxide particles and a 1" centerbody with a 35 degree swirler and three inch quartz tube.

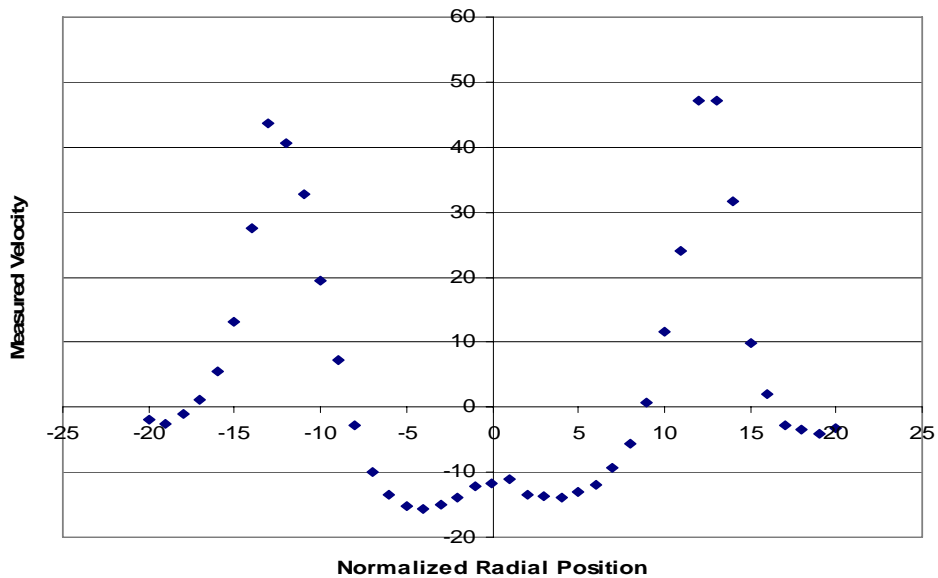


Figure 32: Axial Velocity vs. Normalized Radial Position. Nozzle velocity is 26 m/s corresponding to the 150psi Hotwire cases above. LDV position was at tube exit.

Since the flow field was known, the experimental data from the optically accessible premixer could be examined for additional information and knowledge about the flashback phenomenon that had been observed in the first premixer configuration using thermocouples to sense flashback. For the optically accessible premixer data, a standard configuration was used for the imaging process (see Figure 33). For the data below, a high speed intensified camera was used in a rolling memory mode, which was triggered by a flashback event, so that the prior 4 seconds of images were saved. These images were taken at 2000fps. During processing, the image was trimmed so

that essentially the cross-section of quartz tube was the only visible area. Figure 34 and Figure 35 showed two colorized flashback occurrences which were captured by the high speed camera for CH₄. The propagation for these cases was clearly in the core region.

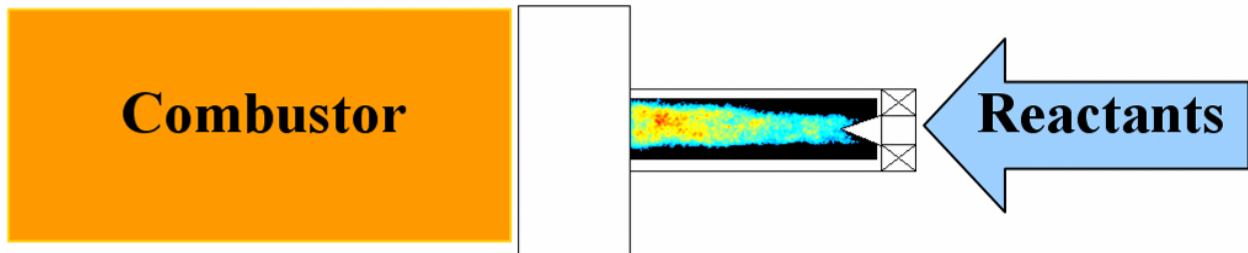


Figure 33: Sample CH₄ flashback image showing the location of the swirler, centerbody, and combustor adapter.

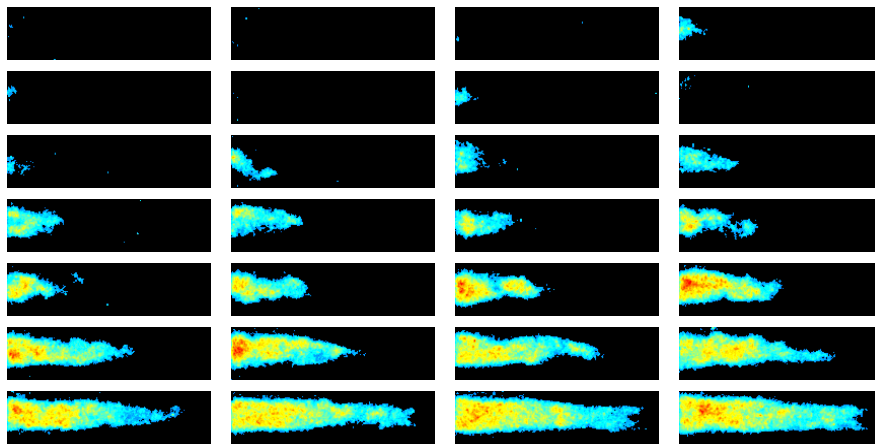


Figure 34: CH₄ Flashback Propagation (Test 1) at 337 K, 1 atm, and nozzle velocity of 39.8 m/s. Shows the flame propagation sequence zoomed in on the quartz tube [Images are 0.5 ms apart].

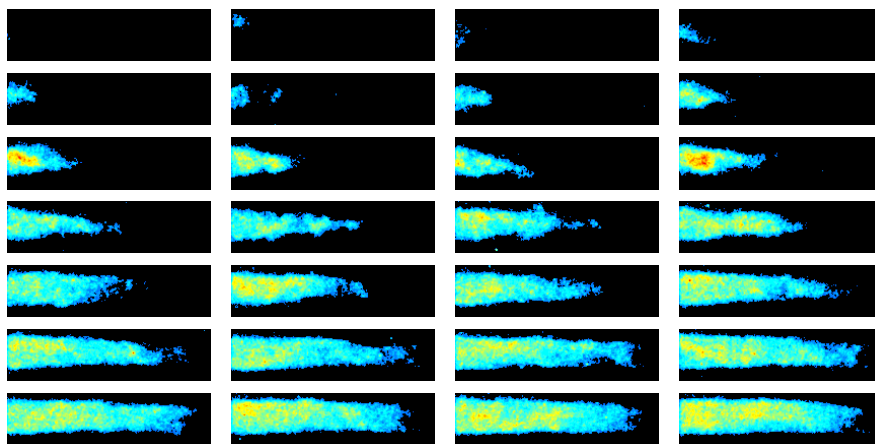


Figure 35: CH₄ Flashback Propagation (Test 2) at 337 K, 1 atm, and nozzle velocity of 39.8 m/s. Shows the flame propagation sequence zoomed in on the quartz tube [Images are 0.5 ms apart].

Moreover, from these images the position of the flame tip was determined as a function of time. This allows for an assessment of the speed of propagation of the leading edge of the flame. Figure 36 plots this flame position vs. time for the two test cases illustrated above. A best fit line through these data shows that the flame was propagating upstream at a speed of 6 and 6.3 m/s, respectively, for these two cases. A third test was also performed at this same condition to check for repeatability, which also had essentially the same flashback velocity. For both cases, the average flow velocity in the nozzle was 40 m/s and air temperature/pressure were 337K and 1 atm, respectively.

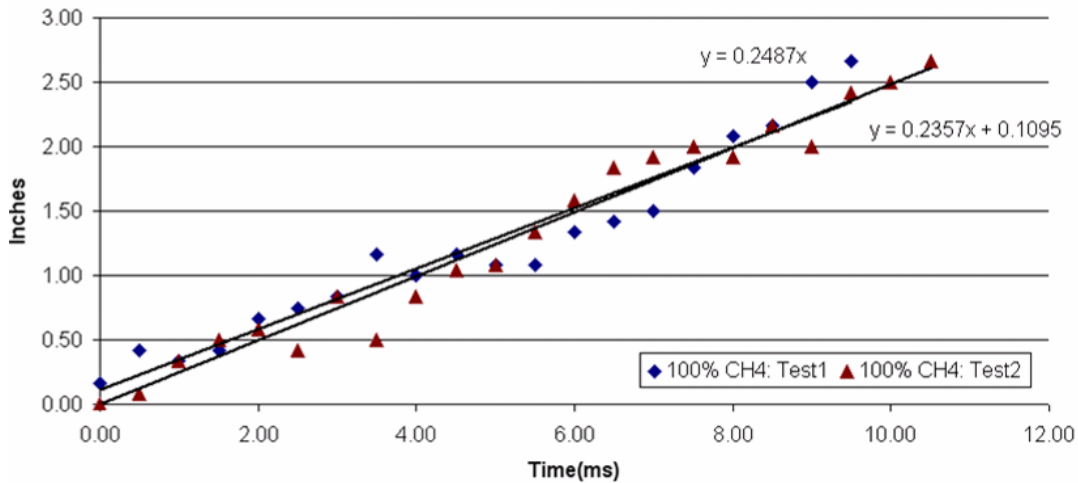


Figure 36: Flame tip position versus time [position in inches, time in ms, and position = 0in was at the inlet to the propagation tube]. Note flame propagation of 6 and 6.3 m/s, respectively between tests 1 and 2.

Figure 37 and Figure 38 show an image set for a 20/80 H₂/CH₄ mixture. As with the previous images, it is important to notice that the flame propagated back in the core region with high velocity flow between the flame and quartz wall. Given the high mean axial velocity of the flow, about 50 m/s in this case, these data all seem to indicate flashback through the combustion induced vortex breakdown (CIVB) mechanism discussed in earlier sections of this report (reactant temperature was 360 K). Figure 39 plotted the flame position versus time for this case, which yields a flame propagation of 10 m/s for the case just described.

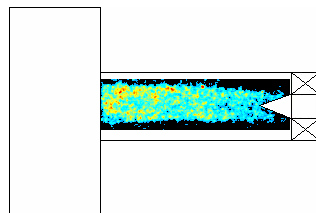


Figure 37: Sample 80% CH₄, 20% H₂ flashback image showing the location of the combustor adaptor, quartz tube, and swirler.

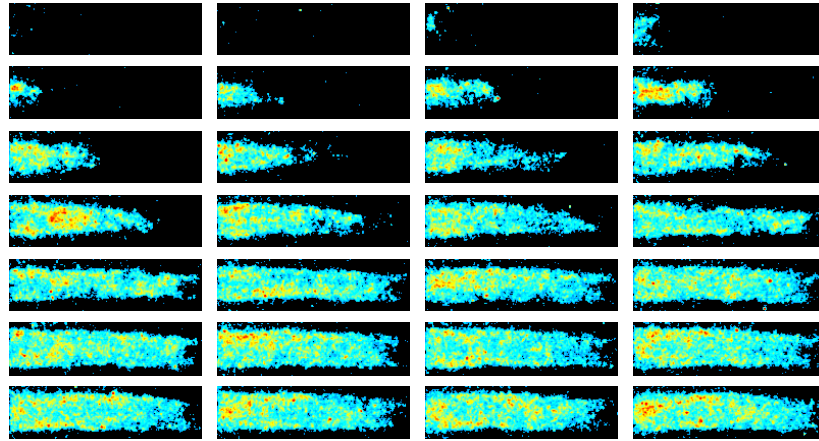


Figure 38: 80% CH₄, 20% H₂ flashback at 359 K, 1 atm, and nozzle velocity of 48.83 m/s. Shows the flame propagation sequence zoomed in on the quartz tube. Images are 0.5 ms apart.

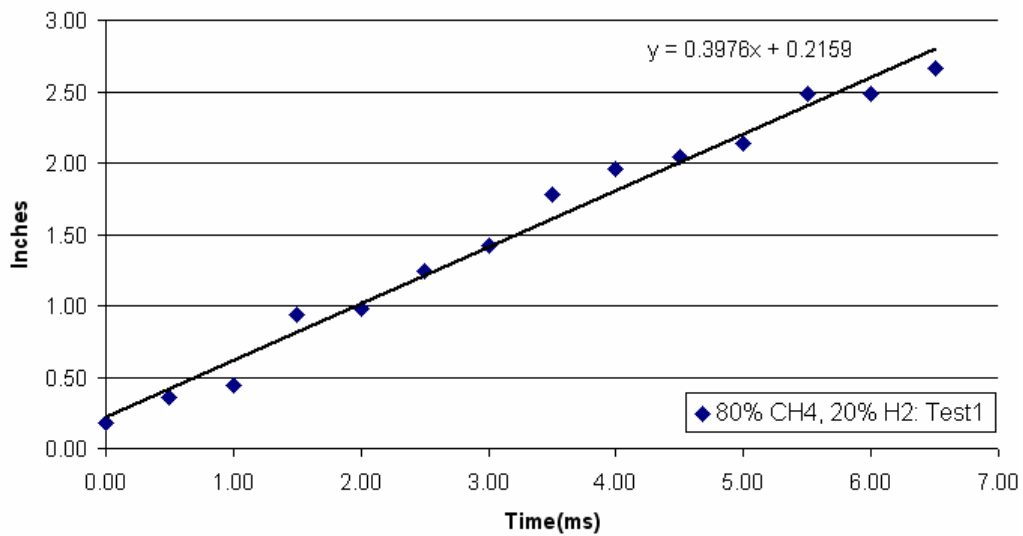


Figure 39: Flame tip position versus time [position in inches, time in ms, and position = 0in was at the inlet to the propagation tube]. Note flame propagation of 10 m/s.

A more careful examination of the movies and flame position results revealed not only the propagation of the flame upstream, but also more complex dynamics. In particular, the flame propagation occurred in a steady fashion for segments of the total flashback occurrence, then “hesitated” slightly, then continued again flashing back through the nozzle. Although not obvious from the frame by frame images shown above, this “hesitation” was very obvious in the movies. It was also very obvious in the flame position vs time graphs; e.g., in the magenta data in Figure 36, this “hesitation” was evident in the flame position staying roughly constant from 2-3 and 7-8 ms. One such event, from 4-5 ms was evident in the blue data as well.

Additional syngas data was taken at 290K and 1 atm using the optically accessible premixer. The focus was on the effect of H₂ on the propagation of the flame. Various amounts of H₂ were added to CH₄ mixtures from 0% to 96%. Figure 40 plots the propagation speed versus amount of H₂ in the fuel mixture. Note that as the H₂ increases, so does the propagation rate for both the lower and higher U_o . For the $U_o = 2$ m/s case, the flame does not stabilize above 80% H₂, the flame would either blowout or flashback into the premixer. It is noteworthy to point out that in Figure 41, the T_{ad} and ϕ are essentially the same for each case, independent of mean nozzle velocity. This gave rise to showing CIVB was the mode of flashback since it has been shown to be driven by temperature and not flame speed. Note though, for the low nozzle velocity case, this trend starts to change with the highest H₂ fuel, this may be showing a change in propagation mechanism. Figure 42 shows the laminar flame speed for these cases. Note that as the amount of H₂ increases, the S_L decreases, giving rise to a potentially non-constant increase of S_T with increased H₂, i.e., showed the great affect of H₂ on fuel properties.

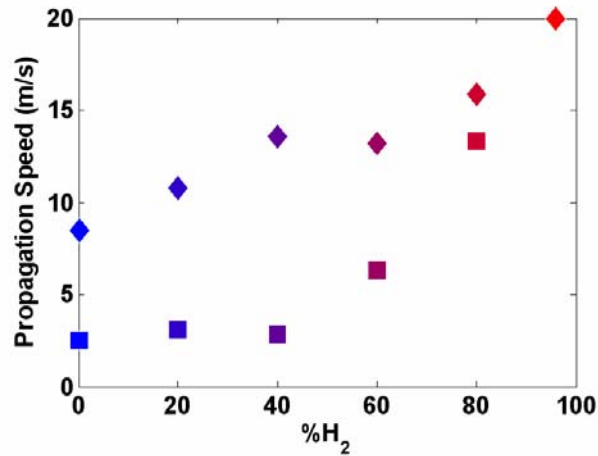


Figure 40: Propagation velocity vs. %H₂ in the fuel for 290K and 1 atm [Note: where squares $U_{nozzle}=18.8$ m/s or $U_o=2$ m/s and diamonds $U_{nozzle}=58.7$ m/s or $U_o=6.5$ m/s].

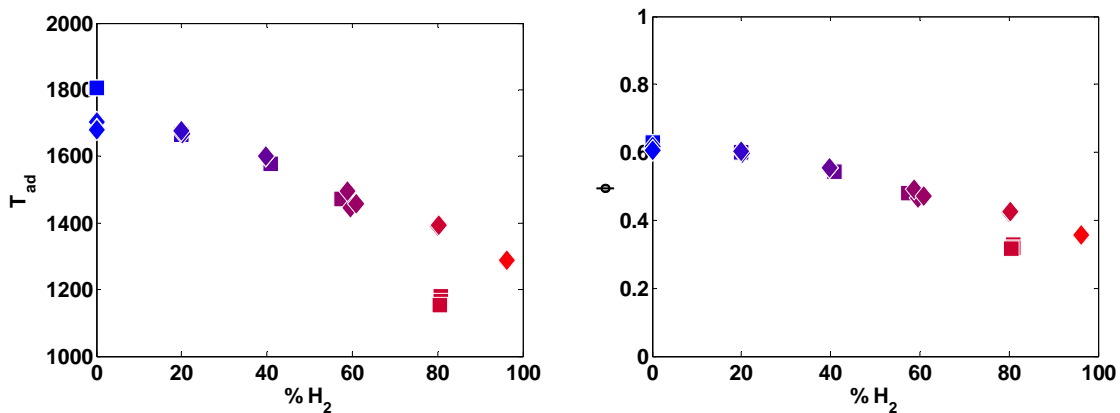


Figure 41: Adiabatic Flame Temperature (K) and equivalence ratio versus percent H₂ for same conditions as tested in the optically accessible nozzle [Note: where squares $U_{nozzle}=18.8$ m/s or $U_o=2$ m/s and diamonds $U_{nozzle}=58.7$ m/s or $U_o=6.5$ m/s].

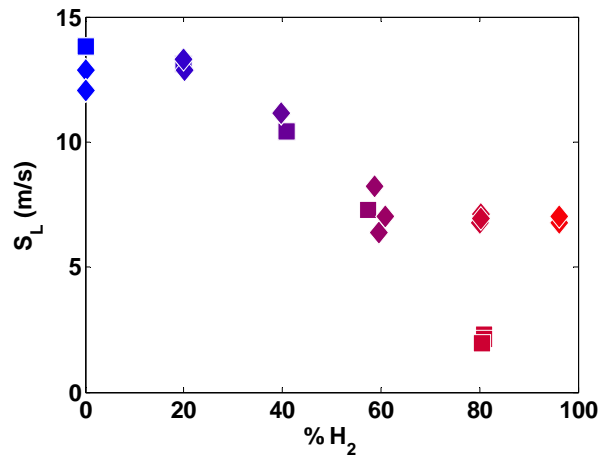


Figure 42: Laminar flame speed versus percent H₂ for same conditions as tested in the optically accessible nozzle [Note: where squares $U_{nozzle}=18.8\text{m/s}$ or $U_o=2\text{m/s}$ and diamonds $U_{nozzle}=58.7\text{m/s}$ or $U_o=6.5\text{m/s}$].

9. CONCLUSIONS

One of the key conclusions of this study is that there exists multiple mechanisms which lead to flashback, each with different underlying parametric dependencies. Counter-intuitively, the percentage of hydrogen had far less effect on flashback characteristics, at least for fuels with hydrogen mole fractions less than 60% and for lower combustor pressures. This was due to the fact that two mechanisms of “flashback” were noted: rapid flashback into the premixer, presumably through the boundary layer, and movement of the static flame position upstream along the centerbody. The former and latter mechanisms were observed at high hydrogen and/or higher combustor pressures, and low hydrogen concentrations, respectively. In the latter mechanism, flame temperature, not flame speed, appeared to be the key parameter describing flashback tendencies. We suggested that this was due to an alteration of the vortex breakdown location by the adverse pressure gradient upstream of the flame. As such, a key conclusion was that classical flashback scalings derived from, e.g., Bunsen flames, may not be relevant for some parameter regimes found in swirling flames. Moreover, with higher pressure tests, it was found that rapid flashback became dominant regardless of the H₂ levels in the fuel. Finally, it was found that in cases of higher pressure/temperature, pure H₂ flames could not be stabilized, i.e., the flame would either flashback or blowout at ignition. This result could have significant implications on the development of future high hydrogen turbine systems.

10. REFERENCES

-
- [1] Kroner, M., Fritz, J., Sattelmayer, T., “Flashback Limits for Combustion Induced Vortex Breakdown in a Swirl Burner,” *ASME Paper # GT-2002-30075*.
 - [2] Durbin, M., Ballal, D., “Studies of Lean Blowout in a Step Swirl Combustor,” *J. Engr. Gas Turbines and Power*, Vol. 118, 1996.
 - [3] Barlow, R.S., Fiechtner, G.J., Carter, C.D., Chen, J.Y., “Experiments on the Scalar Structure of Turbulent CO/H₂/N₂ Jet Flames,” *Comb. Flame*, Vol. 120, 2000.
 - [4] Correa, S.M., Gulati, A. “Non-premixed Turbulent CO/H₂ flames at local extinction conditions,” *Proc. Comb. Inst.* Vol. 22, 1988, pp. 599-606.
 - [5] Drake, M.C., “Stretched Laminar Flamelet Analysis of Turbulent H₂ and CO/H₂/N₂ Diffusion Flames,” *Proc. Comb. Inst.*, Vol. 21, 1986, pp. 1579-1589.
 - [6] Correa, S.M., Gulati, A., Pope, S.B., “Assessment of a Partial Equilibrium/Monte Carlo Model for Turbulent Syngas Flames,” *Comb. Flame*, Vol. 72, 1988, pp. 159-173.
 - [7] Masri, A. R., Dibble, R. W., “Spontaneous Raman Measurements in Turbulent CO/H₂/N₂ Flames Near Extinction,” *Proc. Comb. Inst.* Vol. 22, 1988, pp. 607-618.
 - [8] Maloney, D., “The Simulation Validation Project at NETL,” *DOE Report*, 2002.

-
- [9] Schefer, R. W., "Hydrogen Enrichment for Improved Lean Flame Stability," *International Journal of Hydrogen Energy*, 28, 2003, pp. 1131-1141.
- [10] Wicksall, D., Agrawal, A., "Effects of Fuel Composition on Flammability Limit of a Lean, Premixed Combustor," *ASME Paper #2001-GT-0007*.
- [11] Wohl, K., "Quenching, Flash-Back, Blow-Off Theory and Experiment," *4th Symposium (Int.) on Combustion*, 1952, pp. 69-89.
- [12] Putnam, A., and Jensen, R., "Application of Dimensionless Numbers to Flash-Back and Other Combustion Phenomena," *3rd Symposium on Combustion, Flame, and Explosion Phenomena*, 1948, pp. 89-98.
- [13] Plee, S. L., and Mellor, A. M., "Review of Flashback Reported in Prevaporizing/Premixing Combustors," *Combustion and Flame*, Vol. 32, 1978, pp. 193-203.
- [14] Fritz, J., Kroner, M., and Sattelmayer, T., "Flashback in a Swirl Burner with Cylindrical Premixing Zone," *Proceedings of ASME Turbo Expo 2001*, June 4-7, 2001.
- [15] Kroner, M., Fritz, J., and Sattelmayer, T., "Flashback Limits for Combustion Induced Vortex Breakdown in a Swirl Burner," *Proceedings of ASME Turbo Expo 2002*, June 3-6, 2002.
- [16] Kiesewetter, F., Kirsch, C., Fritz, J., Kroner, M., and Sattelmayer, T., "Two-Dimensional Flashback Simulation in Strongly Swirling Flows," *Proceedings of ASME Turbo Expo 2003*, June 16-19, 2003.
- [17] Thibaut, D., and Candel, S., "Numerical Study of Unsteady Turbulent Premixed Combustion: Application to Flashback Simulation," *Combustion and Flame*, Vol. 113, 1998, pp. 53-65.
- [18] Davu, D., Franco, R., Choudhuri, A., Lewis, A., "Investigation on Flashback Propensity of Syngas Premixed Flames," *AIAA Paper # 2005-3585*.
- [19] Rusak, Z., *Personal Communications*, 2006.
- [20] Wang, S. and Rusak, Z., "The dynamics of a swirling flow in a pipe and transition to axisymmetric vortex breakdown," *Journal of Fluid Mechanics*, Vol. 340, 1997, pp. 177-223.
- [21] Williams, F., *Combustion Theory*, Addison Wesley Publishing Co., 2nd Ed., 1985.
- [22] Zhang, Q., Noble, D.R., Meyers, A., Xu, K., Lieuwen, T., "Characterization Of Fuel Composition Effects In H₂/CO/CH₄ Mixtures Upon Lean Blowout," *ASME Paper # GT2005-689017*.
- [23] Brown, G., Lopez, J., "Axisymmetric Vortex Breakdown Part 2: Physical Mechanisms," *J. Fluid Mech.*, Vol. 221, pp. 553-576.